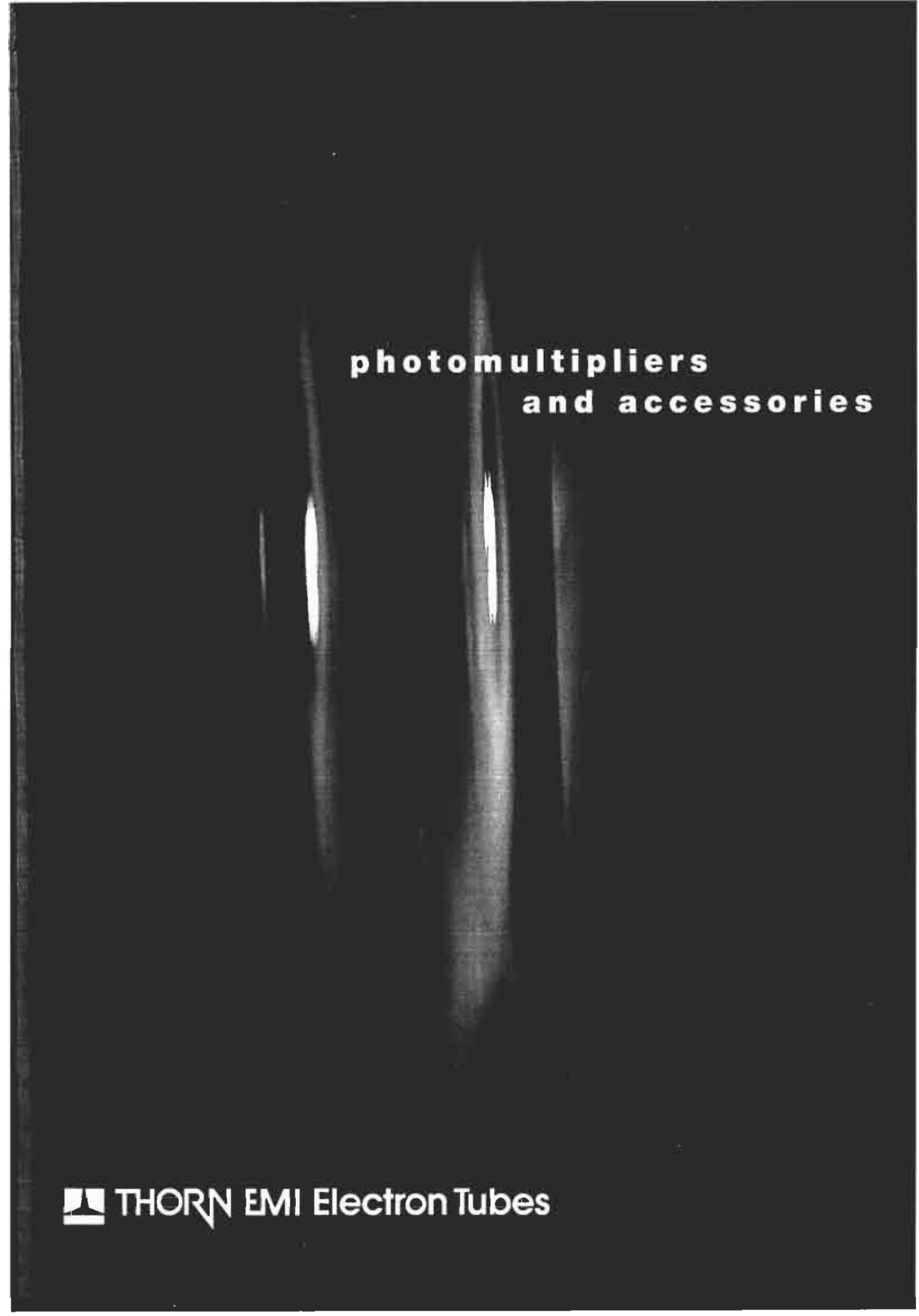
photomultipliers
and accessories
THORN EMI Electron Tubes

Contents

The Photomultiplier and its Operation

Photomultiplier Characteristics

Accessories and Systems

The Photomultiplier and its Operation

1 Introduction

This introduction is intended to provide an understanding of photomultiplier performance and guide designers to the correct choice for their applications. Final selection should be confirmed in consultation with THORN EMI or its international representatives who will advise on the latest developments.

2 Principles of Operation

Photomultipliers are extremely sensitive light detectors providing a current output proportional to light intensity. They are used to measure any process which directly or indirectly emits light. Large area light detection, high gain and the ability to detect single photons give the photomultiplier distinct advantages over other light detectors.

The photomultiplier detects light at the photocathode (k) which emits electrons by the photoelectric effect. These photoelectrons are electrostatically accelerated and focused onto the first dynode (d_1) of an electron multiplier. On impact each electron liberates a number of secondary electrons which are, in turn, electrostatically accelerated and focused onto the next dynode (d_2). The process is repeated at each subsequent dynode and the secondary electrons from the last dynode are collected at the anode (a). The ratio of secondary to primary electrons emitted at each dynode depends on the energy of the incident electrons and is controlled by the inter-electrode potentials. By using a variable high voltage supply and a voltage divider network, to provide the inter-electrode voltages, the amplitude of photomultiplier output can be varied over a wide dynamic range.

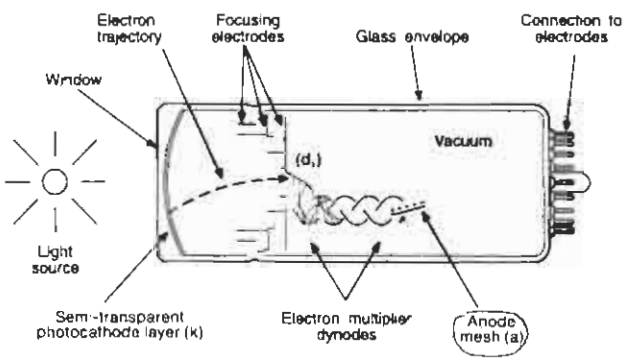

Figure 1

Illustrating the operation of a photomultiplier.

3 The Photocathode

This section gives information on:

- the light sensitive area of the photomultiplier
- the effect of the window on light transmision
- photocathode spectral response
- photocathode sensitivity units

3.1 Photocathode Active Area

Photomultipliers are offered in a range of geometries and sizes to cover applications involving both remote and directly coupled light sources. In end window photomultipliers, the photocathode is deposited as a semitransparent layer directly on the inside of the window. In the majority of types the active area has a circular geometry (Figure 2a). Some have a reduced active area, achieved by electrostatic focusing, which can be an advantage in the detection of very weak light sources (Figure 2b). Special photocathode geometries,(Figures 2 c, d and e), have been introduced for large volume, extended area and large solid angle applications.

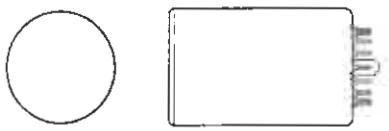

a) Circular

Range of diameters available to suit diffuse and directly coupled light sources.

Application: General purpose; scintillation.

b) Reduced

Electrostatically reduced diameter for minimum dark count.

Application: Photon counting and laser light detection.

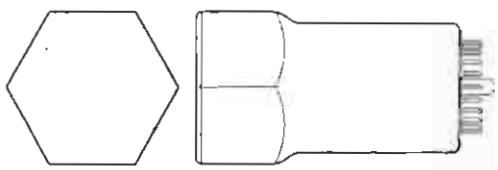

c) Hexagonal

Close packing allows maximum coverage of large areas.

Application: Gamma Camera.

d) 2π

Side wall sensitivity allows wide angle detection.

Application: Probes for radiation monitoring.

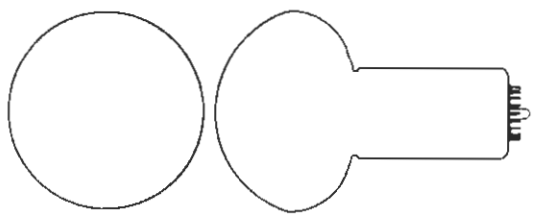

e) Hemispherical

For diffuse light sources, e.g. arrays of photomultipliers.

Application: Fundamental scientific research.

f) Side Window

Matches exit slit, for example, of prism/grating monochromator
Application: Spectrophotometers and photometers.

Figure 2

Various photomultiplier geometries are available and the light sensitive areas are shown coloured; a) through e) are end window types. f) is a side window type where the photocathode is separate from the envelope.

Side window photomultipliers (Figure 2f) have the photocathode deposited on a metallic substrate mounted within the envelope. These have a rectangular area 24x8 mm.

3.2 Window Material

The optical transmission of the window influences the spectrum of light reaching the photocathode. The window material is particularly important when measuring UV light. Certain applications, such as low level scintillation counting, also require window material free from naturally occurring radioactive contaminants. Photomultipliers are manufactured with the following window materials.

Borosilicate glass This is suitable for incident light of wavelength greater than 300 nm. For critical applications, low background borosilicate glass is also available.

UV glass This is used predominantly for side window photomultipliers. The UV cut-off is approximately 185 nm.

Quartz Made from fused silica, this material transmits down to 160 nm and has the added advantage of low radioactive background.

Magnesium Fluoride MgF_2 transmits ultraviolet radiation down to 115 nm and is free from radioactive contaminants.

Sapphire Al_2O_3 is used in metal-ceramic photomultipliers for harsh environments. It has good UV transmission and low background.

The transmission properties of these materials are shown in Figure 3.

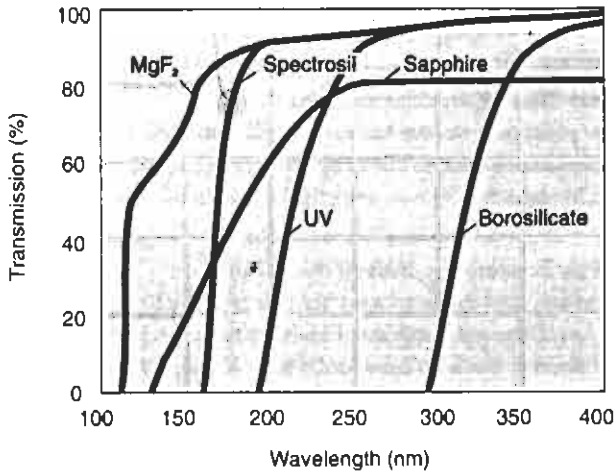

Figure 3

Typical UV transmission curves for windows used in the manufacture of THORN EMI photomultipliers.

3.3 Photocathode Types

Photocathodes can be manufactured from a variety of compounds and each type has a characteristic spectral response. The best choice is usually the one with the maximum response over the wavelength region of interest.

There are other considerations, such as operation at high light levels and thermionic emission which are covered in detail elsewhere. (See Table 5.3(a) and Figure 23).

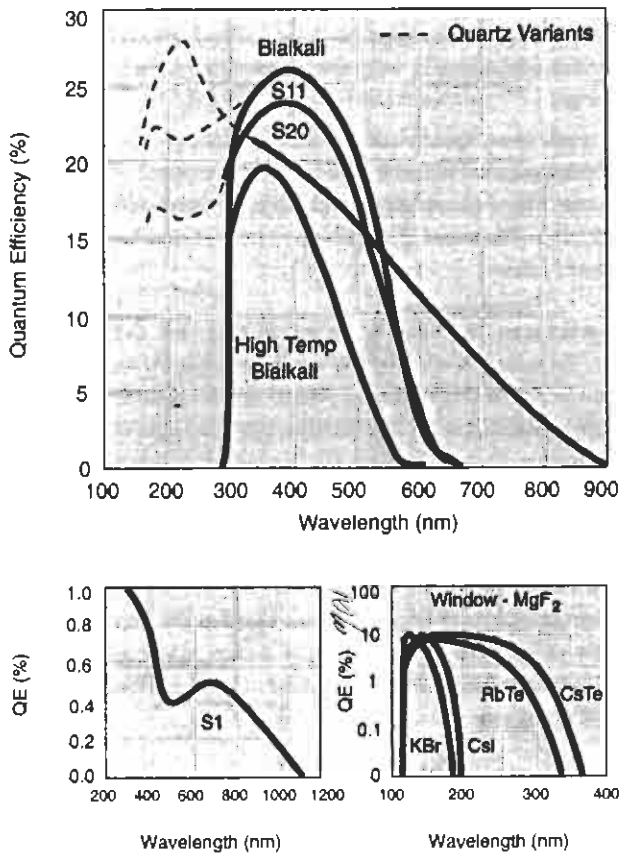

Figure 4

Typical spectral response curves for 52 mm diameter photomultipliers.

Photocathode materials and designations used in THORN EMI photomultipliers are :

i) **Solar Blind** (KBr, CsI, RbTe, CsTe)
These photocathodes are sensitive to VUV and UV light only – hence the terminology. The long wavelength response for KBr and CsI cuts off at 200 nm while RbTe and CsTe extend to 350 nm.

ii) **High Temperature Bialkali** (Na-K-Sb)
Recommended for operation at high temperature because of its very low thermionic emission. This photocathode also finds application in low level light detection.

iii) **S11** (SbCs)
One of the earliest photocathodes with a spectral response covering the ultraviolet and visible range.

iv) **Bialkali** (Sb-K-Cs, Sb-Rb-Cs)
This photocathode has mostly superseded the S11, offering better blue response and lower thermionic emission.

v) **S20 Trialkali** (Na-K-Sb-Cs)
The multialkali photocathode response extends from the UV to near infra-red. It has high light level capability but may require cooling to reduce dark current.

vi) **S1** (Ag-O-Cs)
The S1 sensitivity extends to 1100 nm. Its infra-red response exceeds that of the GaAs types, and it is invariably cooled.

3.4 Photocathode Sensitivity

Photocathode sensitivity describes the conversion efficiency for photons into photoelectrons; the relationship between photocathode sensitivity and wavelength is called the spectral response.

The terms quantum efficiency, radiant sensitivity, luminous sensitivity are used to specify photocathode response. The optimum way of quantifying a photocathode depends on the application. The terms used and their inter-relationship are discussed below.

Quantum Efficiency: η (λ) or QE%

η (λ), the quantum efficiency at wavelength λ is the average photoelectric yield per incident photon and is normally expressed as a percentage. It is the most fundamental unit concerning the performance of the photomultiplier. Important practical considerations such as resolution, signal/noise and detectivity are all related to quantum efficiency.

Radiant Sensitivity E(λ) or QE%

Radiant sensitivity or responsivity is defined as the photocathode current emitted per watt of incident radiation at wavelength λ and is expressed in mA/W. It is related to quantum efficiency in the following way:

$$E(\lambda) = \frac{\lambda \eta(\lambda)}{1.24} \quad mA/W \qquad \ldots(1)$$

provided that λ is expressed in nanometres.

For example, a QE of 25% at 400 nm is equivalent to a radiant sensitivity of 80.7 mA/W.

Luminous Sensitivity: S

S is the most relevant specification for light sources which have a spectral response corresponding to that of the human eye. The human eye is sensitive to electromagnetic radiation between 400 and 760 nm and its relative luminous efficiency V(λ) has been agreed internationally.

One of the standard calorimetry illuminants, a tungsten filament lamp operated at a colour temperature of 2856 K, is used as the light source. This approximates to a black body radiator at the same temperature and has a known radiant power spectrum I(λ)dλ W/m.

The relationship between the photocathode luminous sensitivity S, η(λ), I(λ) and V(λ) is as follows :

$$S = \frac{10^3 \int_0^\infty I(\lambda)\lambda\eta(\lambda)\, d\lambda}{1.24 \times 680 \int_0^\infty I(\lambda)\, V(\lambda)\, d\lambda} \quad \mu A/lm \qquad \ldots(2)$$

For a particular photocathode, S is calculated from measured values of η(λ) and tabulated values of I(λ) and V(λ) by integration.

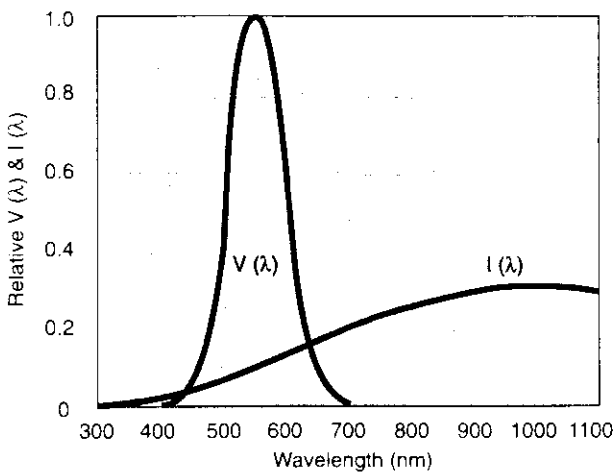

Figure 5
Relative luminous efficiency of human eye V(λ) and radiant power of a tungsten filament lamp operated at 2856 K.

The luminous sensitivity specification has been adopted by all photomultiplier manufacturers. Values of S range from 20 μA/lm to over 400 μA/lm, depending on the photocathode type. In the THORN EMI test the lamp output is adjusted to 1 millilumen and approximately 80% of the photocathode area is illuminated.

Filter Measurements (CB, CR, IR)

It is clear from (2) that S is derived by integrating terms which are wavelength dependent, with a high contribution coming from long wavelengths. Luminous sensitivity figures cannot therefore be used to compare photocathode types with appreciably different

spectral responses. In other words, because it refers to white light, S is not necessarily a good selection parameter. By using specific colour filters placed between the standard light source and the photomultiplier, the usefulness of S has been extended.
For practical purposes photocathodes are thus individually characterised by noting the response to filtered light from a white light source. The filters used are standard throughout the industry with transmission characteristics selected to match the entire range of photomultiplier applications. The filters characterised in Figure 6 reflect the fact that photomultiplier applications tend to divide into blue light, red light and infra-red light. Filter measurement results are recorded on the test ticket supplied with each tube, as illustrated in Figure 13.

Grading and selection with these filter measurements have become standard practice. The filters of Figure 6 are as follows:

Corning Blue (CB)

A Corning CS-5-58 filter, of half stock thickness, is used for this measurement. Corning Blue values range from abour 5 to 16 and are a useful relative measure of sensirivity for sources emitting in the blue region of the spectrum. This filter is most relevant to photomultipliers with bialkali photocathodes.

Corning Red (CR)

A Corning CS-2-62 filter provides the Corning Red value and is appropriate for selecting photomulripliers intended for sources emitting in the red and near IR regions of the spectrum.

Infra Red (IR)

A Wratten 87 filter is used to select S20 phorocarhodes for applications requiring response in IR region of the spectrum.

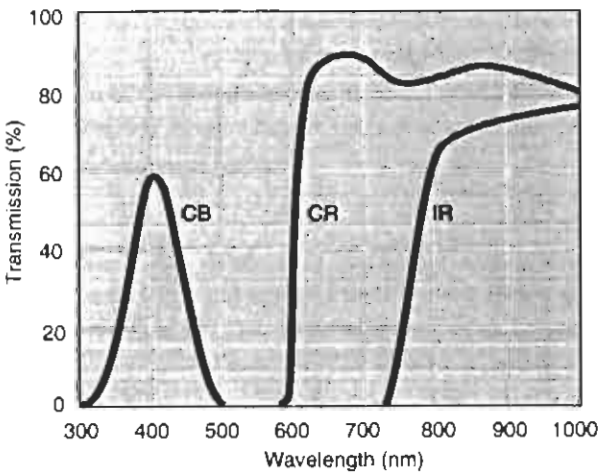

Figure 6
Filter transmissions.

Cathode QE% Measurement

THORN EMI has spectral response equipment which provides tabulated values of quantum efficiency and radiant sensitivity traceable to standards calibrated at the National Physical Laboratory, England. Spectral response is measured with 360 V between k and d_1 and with all other electrodes connected to d_1. Approximately 80% of the photocathode area is illuminated in this test.

This calibration is available to customers as an option. Values can be provided at any wavelength which is a multiple of 10 nm within the range 110 nm and 1100 nm.

The calibration also provides values of S, CB, CR and IR.

Effective Diameter and Uniformity

The effective cathode diameter is governed by the inner diameter of the glass envelope and the electron optical design (refer to data sections for nominal values). The output from THORN EMI photomultipliers is examined using a flying spot scanner to check uniformity as illustrated in Figure 7. Ideally, the output from the photomultiplier should be independent of the point of illumination on rhe photocathode but in practice there is variation over the active surface. This arises from:

- spatial variation in the sensitivity of the photocathode, particularly in the side window types
- variation in the angle of incidence and point of impact of photoelectrons on the firsr dynode, resulting in variation of secondary electron emission

Some photomultipliers include a focus electrode (f) to allow individual trimming of overall uniformity. The optimum $V(f\text{-}d_1)$ and $V(k\text{-}d_1)$ settings are included on the test ticket.

In critical applications, diffusing the incident light over the photocathode may be beneficial. THORN EMI can provide photomultipliers with a vapour blasted entrance window to special order.

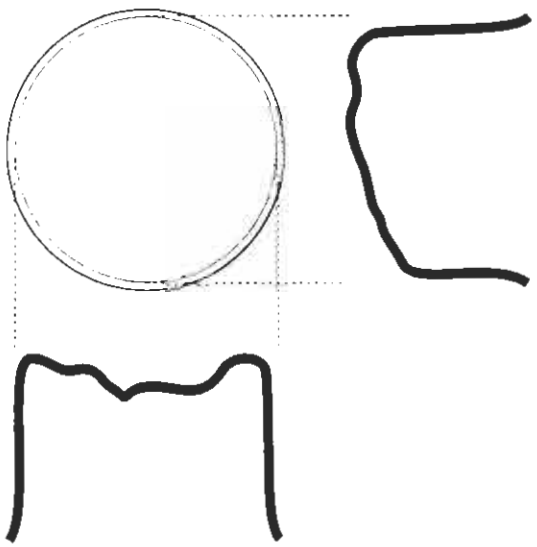

Figure 7
Typical flying spot uniformity scans for a 2" photocathode. The spot size is 2mm.

4 The Electron Multiplier

The electron multiplier is a very low noise, high gain, wideband amplifier with the capability of providing an output compatible with the sensitivity of available instrumentation.

The attributes of the range of structures and active surfaces that are used in THORN EMI photomultipliers are discussed in **4.2**.

4.1 Input Region

Photoelectrons must be accelerated and focused onto an active area of the first dynode. The design of the k-d_1 region has been optimised to maximise the collection of photoelectrons from the entire photocathode area, as illustrated in Figure 8. Some photomultiplier types have a separate focus electrode in the k-d_1 region which can be used:

- to maximise the photomultiplier output from non-uniform light sources
- to gate the photomultiplier on or off [1]

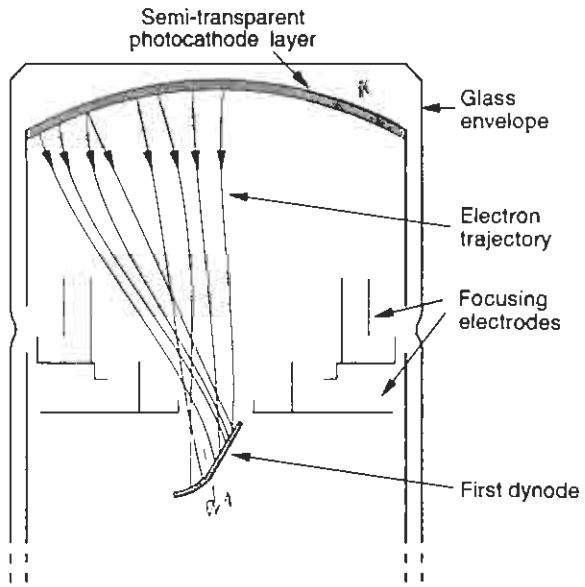

Figure 8

Photoelectron trajectories between photocathode and first dynode.

4.2 Types of Multiplier Structure

A number of multiplier structures is available. Generally the various structures represent a compromise between physical size and electrical performance, particularly with reference to gain, timing, linearity, and immunity from external magnetic fields. Table 4.2 summarises these attributes and indicates the relative merits of individual structures.

Table 4.2

Ranking of the attributes of multiplier structures.
Four ticks represents highest ranking.

Structure	Size	Gain	Timing	Linearity	Magnetic Immunity
	Compact	Maximum	Fastest	Best	Best
Venetian Blind (VB)	√√	√√√	√√	√√	√√
Compact Focus (CF)	√√√√	√	√√√	√√√	√√√√
Box and Grid (BG)	√√√	√√	√	√	√√√
Linear Focus (LF)	√	√√√√	√√√√	√√√√	√

4.3 Secondary Emission Surfaces

Two secondary emitting surfaces are available - oxidised beryllium copper (BeCu) and caesiated antimony (SbCs). In some cases there is an option of dynode material available. The choice of dynode material should be governed by the nature of the application. The principal properties are summarised in Table 4.3.

Table 4.3

Performance comparisons of secondary emission surfaces.

SbCs Dynodes	BeCu Dynodes
● high gain/volt	● best linearity (dynamic range)
● low rate effect	● high temperature operation
● best temperature coefficient	
● best gain stability	
● best hysteresis	

4.4 Gain

Gain in a photomultiplier is derived by current amplification. Each dynode amplifies the incident electron current and the overall gain is given by the product of the individual dynode contributions. With many stages of gain, a small photoelectric signal is amplified to a measurable level. Denoting the gain of the first dynode as δ_1, and so on, the final current at the anode, for a photomultiplier with n dynodes is:

$$I_a = \delta_1 \delta_2 ... \delta_{n-1} \delta_n I_k \qquad ...(3)$$

or

$$I_a = G I_k \qquad ...(4)$$

where I_k and I_a are the photocathode and anode currents respectively. G is the photomultiplier gain.

The gain of each dynode is related to the energy of the incident electrons and hence to the inter-dynode voltage. The gain of the first dynode is shown in Figure 9 for both BeCu and SbCs surfaces. The gain of each dynode in the photomultiplier follows a similar curve.

In general, a single high voltage power supply is employed with a resistive voltage divider network to provide suitable inter-electrode voltages. The more dynode stages in the photomultiplier, the higher is the gain at a specific overall applied voltage and the higher the maximum gain attainable.

This is illustrated in Figure 10. **It should be noted that gain figures and curves are obtained with a particular voltage distribution specified in this catalogue. The gain curve is different if the voltage distribution is different from that specified.**

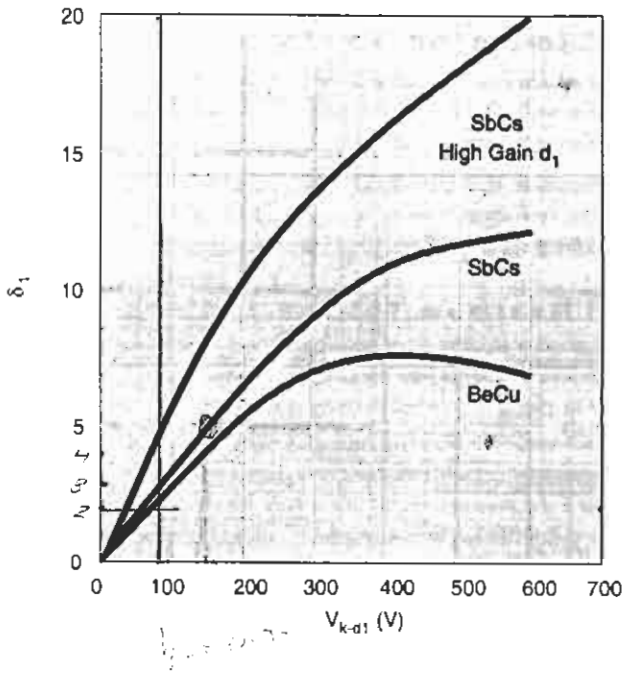

Figure 9
Variation of first dynode gain δ_1 with k-d_1 voltage

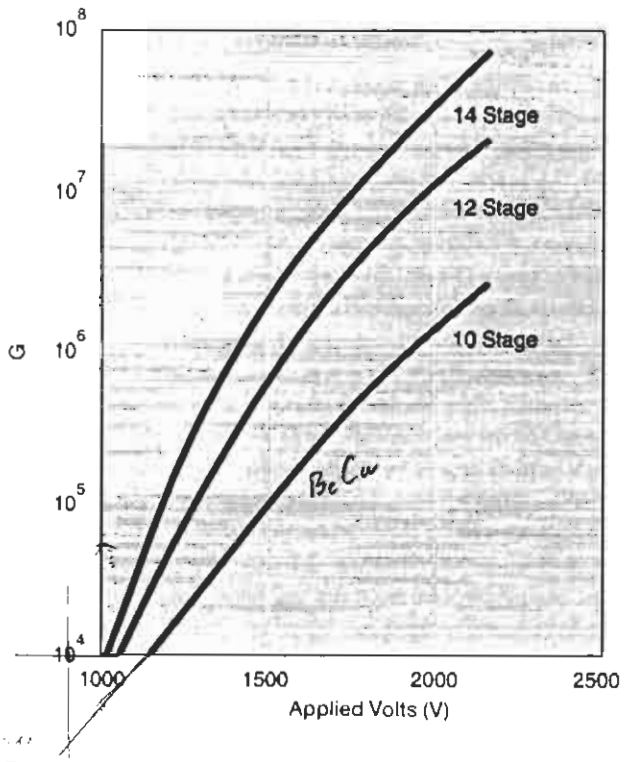

Figure 10
Variation of photomultiplier gain G with applied voltage, illustrating the effect of number of dynode stages.

4.5 Anode Sensitivity A/lm

The voltage required to attain the specified anode sensitivity is recorded on the test ticket. Specified in this way the output is referred to the cathode sensitivity, S, quoted in μA/lm.
The gain can be derived from this and S by using the following relationship:

$$G = \frac{AnodeSensitivity(A/lm)}{CathodeSensitivity(\mu A/lm)} \times 10^6 \quad ...(5)$$

THORN EMI specifies the voltages required on each photomultiplier to achieve two fixed anode sensitivities (the nominal and the maximum) with inter-dynode voltage distributions as specified on page 62. It is sometimes useful to construct a gain-voltage curve using these two points on the appropriate graph given in the Photomultiplier Characteristics section of this catalogue.

4.6 Anode Equivalent Circuit

The equivalent circuit for a photomultiplier is an **ideal current source** in parallel with an output resistance R_0 ($>10^{12}$ Ω) and capacitance C_0 (<10 pF). The measured output depends on the load resistance R_L and capacitance C_L in combination with R_0 and C_0.

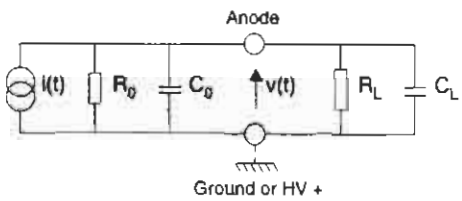

Figure 11
The equivalent circuit for a photomultiplier.

The equivalent circuit applies to both dc and pulsed applications. In the case of pulsed light sources, the nature of the output signal depends upon the time profile of the input. Many applications involve light sources with an exponential profile. The following analysis is useful in order to determine the amplitude and timing profile for such input stimuli:

The time constant of the circuit is: $\tau = RC$,
where:

$$R = \frac{R_0 R_L}{R_0 + R_L}$$

and

$$C = C_0 + C_L \quad ...(6)$$

Consider the output voltage response to a light source which decays with a single exponential time constant, τ_s
then:

$$i(t) = N\,e\,G\,exp\,(-t/\tau_s) \quad ...(7)$$

and

$$v(t) = \frac{N\,e\,G\,R}{\tau - \tau_s}\,[exp(-t/\tau_s) - exp(-t/\tau)] \quad ...(8)$$

where:
N is the number of photoelectrons produced by the light pulse,
e is the electronic charge,
G is the photomultiplier gain.

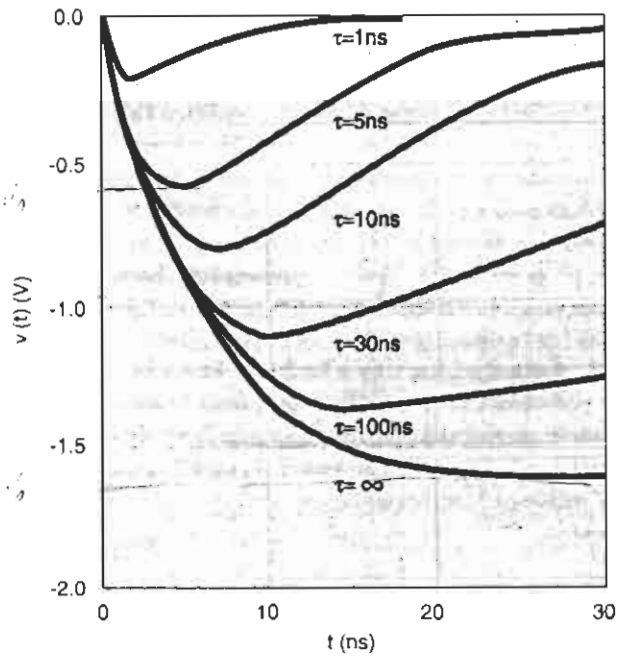

Figure 12

The output v(t) for various time constants, assuming N = 100, G = 1 x 10⁶, τ, = 5 ns, C = 10 pF in Equation (8).

By inspection of (8), the output voltage is a faithful representation of the input current when $\tau << \tau_S$; this is referred to as **current mode operation.** Voltage mode operation applies with $\tau >> \tau_S$, in which case the pulse heighr in volts is proportional to the total input charge. For high or variable pulse rates there is a danger of overlap when operating in voltage mode. It is usual practice to use a value of $1/\tau$ less rhan one quarter of the event rate to avoid pulse pile-up effects. In pulsed light applications the choice of τ depends principally on the characteristic decay time of the light source and the anticipated event rate. For example, in Na(Tl) applications, where τ_S = 230 ns, choosing $\tau \approx 1$ µs ensures good integration of the signal while permitting event rates of up to about 50 kHz, before the onset of serious pile-up effects.

In rhe extreme case $\tau \rightarrow \infty$, C integrates the charge and the output rises with a time constant τ_S and remains there:

$$v_o(t) = \frac{N e G}{C} \left[exp(-t/\tau_S) - 1 \right] \qquad ...(9)$$

There are applications where the output is not pulsed but varies unpredictably with time. In film scanning for example, a transition from light to shade gives a step change in ourput, measured in microseconds. Here the consideration is one of choosing the output time constant to match the fastest anticipated transition, while simultaneously providing some smoothing of unwanted statistical fluctuations. For example, if the fastest transition t, has a time constant of 1 µs and if $(C_o+C_i)R_L$ is chosen to be $<3 \times 10^{-7}$, the output circuit will reproduce the rransition quite fairhfully. For R_L=10 kΩ, for example, (C_o+C_i) needs to be ≤30 pF. With this time constant, transitions faster than 100 ns will not be followed.

5 Limits on Performance

Photomultipliers are high gain, wide bandwidth, optical detectors and, as with all such sensors, limitations apply to the quality of performance with regard to:

- maximum gain (sensitivity)
- time or frequency response
- linearity of response
- dark current
- stability and hysteresis
- noise-in-signal

5.1 Maximum Voltage and Sensitivity

The photomultiplier must not be operated beyond the maximum recommended sensitivity specified in this catalogue. Beyond this limit feedback effects may become significant, resulting in unstable performance and high dark current with the possibility of breakdown under extreme conditions. Permanent damage will occur if the photomultiplier suffers breakdown. The sensitivity limit is determined by the maximum allowable gain of the multiplier, which depends on the type of multiplier structure. The maximum allowable inter-electrode voltages are determined by the spacing of the electrodes in the photomultiplier. Excessive voltage causes electrical breakdown and this must be borne in mind in voltage divider network design (Section 8). Similarly, the maximum allowable overall voltage is limited to less than the sum of the stated maximum inter dynode voltages. Maximum allowable inter- electrode voltages are given for each tube type in the Photomultiplier Characteristics section of this catalogue.

The THORN EMI test ticket, an example of which is shown in Figure 13, is supplied with every photomultiplier. This gives the maximum recommended sensitivity and rhe overall voltage at which this is achieved using the standard voltage divider distribution used for testing (These are listed on page 62 of rhis caralogue). If a voltage distribution other than that used by THORN EMI is chosen, the overall voltage required ro achieve rhe maximum overall sensitivity will be different.

5.2 Time Response

The response of rhe photomultiplier to a delta pulse of light is governed by the electron trajectories within the tube. Photoelectrons created by the light pulse follow individual paths to rhe first dynode, depending on their point of origin on the photocathode and on their emission velocities. It follows that they land on the first dynode at different points and at different times. Secondary electrons travel individual paths between dynodes, causing further time dispersion. The phoromultiplier output pulse is characterised by:

- rise time t_r
- full width at half maximum t(fwhm)
- transir time t_t

These parameters are defined in Figure 14.

Bandwidth is not usually quoted for photomultipliers, although it can be derived from the approximate formula:

$$\Delta f\,(3dB) = \frac{1}{3t_r} \quad Hz \qquad ...(10)$$

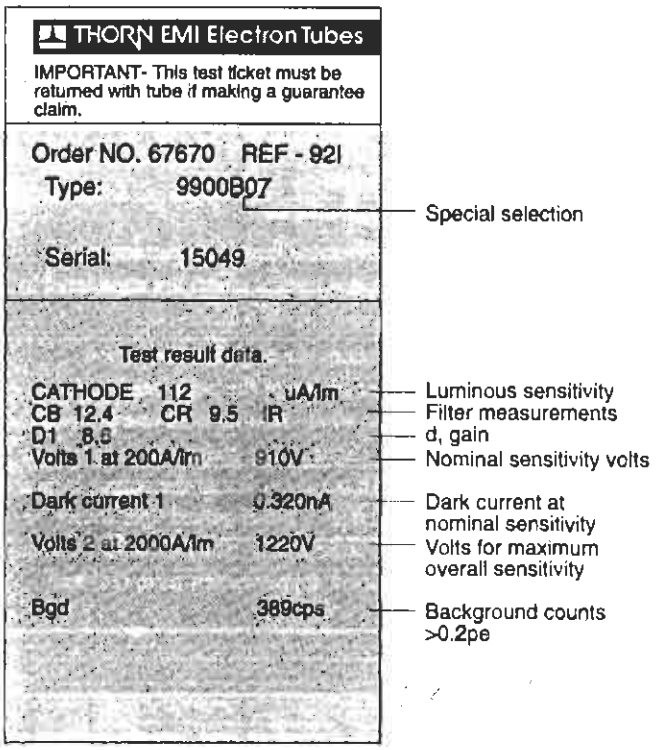

Figure 13

Sample photomultiplier test ticket. Parameters are measured using standard voltage dividers, listed on page 62.

The variation in transit time from one light pulse to the next is a critical parameter when using photomultipliers to detect the time occurrence of events. The standard deviation, σ, derived from a large sample of events gives the transit time jitter (sometimes the fwhm of the distribution, equal to $\sim 2.36\sigma$, is quoted as the transit time jitter).

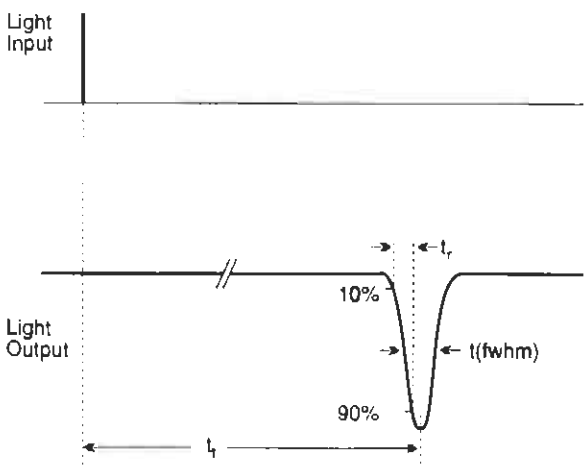

Figure 14

Illustrating photomultiplier time response (rise time, full width at half maximum, transit time).

Photomultipliers with plano-concave windows and linear focused multipliers give the best time performance. Other factors affecting timing include:

- the number of dynodes. Fewer stages give better timing
- the overall voltage. Higher field strengths improve timing. The best timing is attained having high k - d_1 voltage, with operation at the maximum recommended gain. The time response varies approximately as $1/\sqrt{V}$
- the photocathode diameter. Smaller diameters have better timing. The best timing is achieved when illuminating the central area only

Table 5.2 summarises the time response of THORN EMI photomultipliers.

Table 5.2

Timing performance of THORN EMI photomultipliers. Transit time jitter figures refer to single photon excitation.

Structure	Transit Time (ns)	Rise Time (ns)	Transit Time Jitter (σ) (ns)
VB	40-110	8-15	2.2-5.7
BG	50-80	12-18	4.2-6.4
CF, SW	20-35	1.5-2.5	0.5-1.0
LF	20-55	1.8-2.7	0.5-1.2

5.3 Linearity and Maximum Current

a) Direct Current Limits

High mean anode currents cause fatigue effects and reduced photomultiplier lifetime; the maximum mean anode current should be less than 100 µA and most stable performance is achieved by operating below 10 µA. With correct voltage divider design all multiplier structures are linear, within one percent, up to anode currents of 100 µA. Limits on maximum photocurrent also apply, governed by the resistivity of the photosensitive layer. Exceeding these limits results in non- linear performance.

Side window photomultipliers, with a metal substrate supporting the photosensitive layer, can sustain much higher currents than end window types. Photocurrenr limits are given in Table 5.3(a).

Table 5.3(a)

Maximum cathode currents at 20 °C.

Cathode Type	I_k (nA/cm^2)
Bialkali	2.5
High Temperature Bialkali	2.5
S1	5
S11, RbCsSb	15
S20	250
Side Window	5000

b) Pulsed Current Limits

Pulsed anode currents greater than 100 µA can be drawn with the proviso that the mean anode current, averaged over one second, is below 100 µA. The photomultiplier output current will be linear with respect to light input until the onset of space charge effects. The current at which non-linearity first appears depends on the type of multiplier structure and on the operating conditions. Linearity can be improved with a voltage divider distribution which has higher inter dynode voltages on the later stages. Linearity also depends on the dynode secondary emitting surfaces as detailed in Table 5.3(b). Recommended divider distributions are given in Section 8.

Linearity measurements are made using two LEDs and a double pulse generator. Two pulses are applied with the second delayed with respect to the first (individual outputs). Then the two pulses are applied in coincidence (summed output). Non-linearity becomes evident when the summed output pulse differs from the sum of the individual pulses.

Table 5.3(b)

$\hat{i}_a$ is the peak anode current for which there is a 5% departure from linear operation. $V_{d\text{-}d}$ is the interdynode voltage.

Dynode Structure	$\hat{i}_a$ (mA) at $V_{d\text{-}d}$ = 100 V Dynode Surface		$\hat{i}_a$ (mA) at $V_{d\text{-}d}$ = 300 V Dynode Surface	
	CsSb	BeCu	CsSb	BeCu
LF	30	50	100	150
CF	10	20	30	50
VB	2	4	5	20
BG	0.1	0.2	0.5	1

5.4 Noise, Dark Current and Dark Count

For the purpose of analysis it is convenient to categorise photomultiplier applications as

i) continuously variable (sometimes referred to as dc) or
ii) pulsed.

A film scanner is a good example of i): the intensity of the light reaching the photomultiplier is continuously variable over a wide dynamic range and is subject to sudden transitions in level.

The required bandwidth of the associated output circuit and electronics is of the order of 3 MHz in order to follow these fast transitions.

The output produced by a NaI(Tl) crystal has a characteristic decay time of 230 ns, and between events, the photomultiplier output is ideally zero. This is an example of pulsed operation ii).

The purpose of this section is to examine how statistical fluctuations and photomultiplier dark current contribute to non-ideal performance in the two modes of operation i) and ii). An understanding of this will ultimately lead the user to the achievement of best performance through both selection of a tube with the right parameters and operating the chosen device optimally.

Consider a light source which remains constant in intensity over a period of seconds. If the anode output is observed on an oscilloscope, it will be noticed that the trace will always have some fluctuation superimposed upon it. There are two sources causing the fluctuation illustrated in Figure 15:

i) dark current contributions
ii) statistical noise-in-signal effects

The nature of and the contributions from dark current are discussed in Section 5.5 while statistical effects are considered in the next Section, Noise.

In the pulsed mode of operation, the consideration is how faithfully the photomultiplier preserves the pulse height information. In other words, what variation from one pulse to the next can be expected from a light source giving the same output in each light pulse. Figure 16 is a snap-shot of the output from a phoromultiplier illuminated from a steady pulsed light source, in this instance an LED. The statistical contribution to the pulse-to-pulse variation can be predicted approximately from (11) and more correctly, from (14)

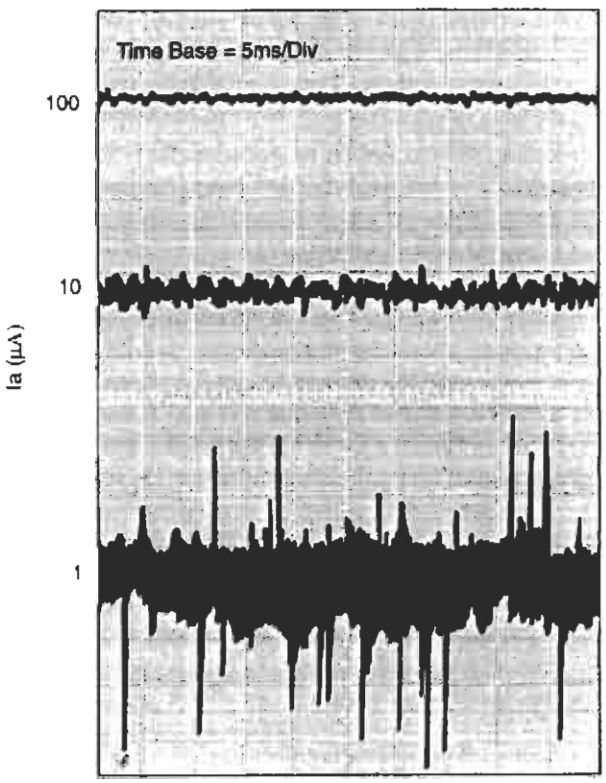

Figure 15

dc Detection: Illustrating the output signal for three different levels of illumination, measured at G = 10^6. The rms noise contribution can be predicted by using the chart in Figure 18.

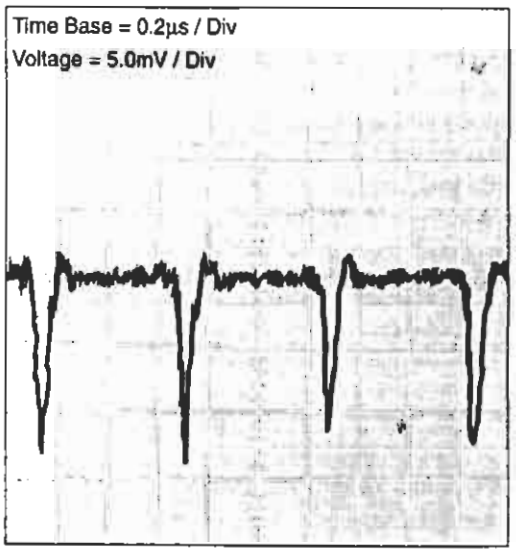

Figure 16

Pulsed Operation. The output from a photomultiplier viewing a pulsed light source set to give 100 photoelectrons, average, per pulse. The fluctuations in area from one pulse to the next are an inescapable manifestation of noise.

A fluctuation in area under each pulse and a fuzziness of the trace is apparent. As before, the two sources of fluctuation i) and ii) contribute. A charge sensitive multichannel analyser can be used to measure the area of each pulse, assigning it to a specific memory location. The result of analysing a sequence of pulses shown in Figure 16 is displayed as a spectrum in Figure 17.

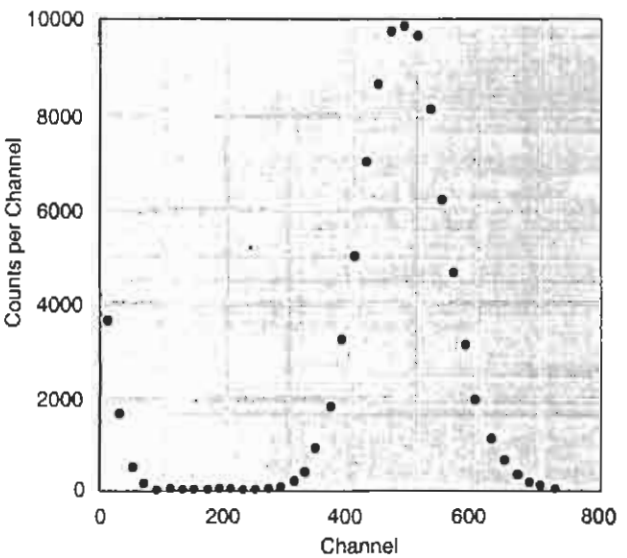

Figure 17

A pulse height distribution measured with a charge sensitive multichannel analyser (MCA). When the photomultiplier views a pulsed light source of constant intensity, there is variation in pulse height from one pulse to the next.

Noise

In common with the measurement of all physical processes, repeated measurement does not always give exactly the same value. In the photomultiplier the variation in output signal is related to the statistical fluctuation in the number of photoelectrons created (photoelectron noise). There is an additional contribution from the statistical variation in the number of secondary electrons created per incident electron on each dynode (multiplication noise). These effects yield expressions for signal-to-noise ratio, (S/N), which can be applied to any detection system using photomultipliers.

Photocathode Noise

Consider a steady light flux incident on the photocathode producing M photoelectrons per second. The photoelectric effect is a quantum mechanical one and is subject to statistical fluctuations described by Poisson statistics. If the photomultiplier output is measured over a period of time T, there will be an average of MT photoelectrons produced. Based on Poisson statistics, the standard deviation associated with MT is $(MT)^{\frac{1}{2}}$. The signal-to-noise ratio is:

$$S/N = \frac{MT}{(MT)^{\frac{1}{2}}} = (MT)^{\frac{1}{2}} \qquad ...(11)$$

If we assume that the gain of the multiplier is ideal, that is, not itself noisy, then at best the output signal will have the fluctuation of (11) imposed on it.

Equation (11) explains the origin of noise-in-signal; in this form it is useful for predicting quantitative performance in pulsed applications. For continuously variable applications, the effect must be treated in a more general way by taking account of the bandwidth of the measuring electronics rather than the sampling time T.

The shot noise formula relates T to the inverse of the bandwidth through the Fourier transform and predicts the noise on a cathode current of I_k as:

$$(\overline{i_k^2})^{\frac{1}{2}} = (2\, e\, I_k\, \Delta f)^{\frac{1}{2}} \qquad ...(12)$$

where for any parallel combination of load resistances R and capacitance C, $\Delta f = 1/4RC$. Again, assuming ideal gain G, the S/N ratio is:

$$S/N = \frac{I_k}{(\overline{i_k^2})^{\frac{1}{2}}} = \frac{I_k}{(2\, e\, I_k\, \Delta f)^{\frac{1}{2}}} \qquad ...(13)$$

Equation (13) is illustrated in Figure 18.

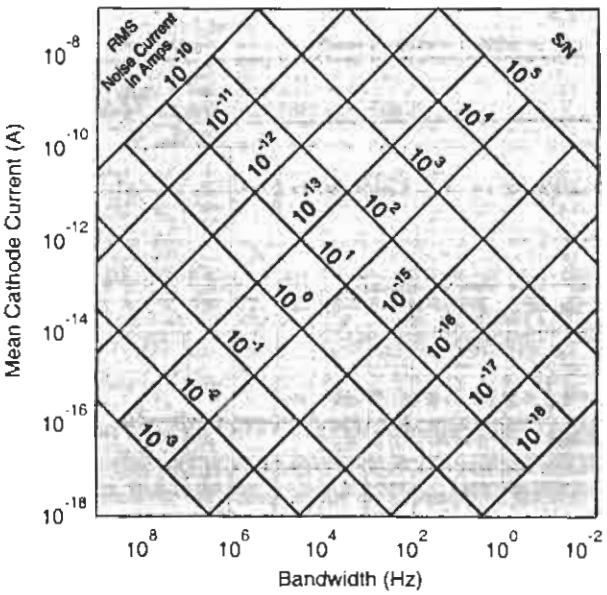

Figure 18

Graphical representation of the shot noise formula. (If the multiplier noise is taken into account, the signal-to-noise ratio read off above should be multiplied by 1/a, as discussed in the Multiplication Noise section).

Referring to a film scanning example, with Δf=3 MHz, if the requirement is S/N≧100, then I_k needs to be $>\sim 10^{-8}$ A. To put this in perspective, for a gain of 10^4, the associated anode current will be 100 μA.

Multiplication Noise

The signal-to-noise ratio is always less than predicted by Equations (11) and (13) because the electron multiplier is non ideal. For any dynode there is a statistical spread in secondary emission coefficient around the mean value $\bar{\delta}$. The statistical effect is of greatest importance at the first dynode, d_1, than at any subsequent dynode. This is because the number of secondary electrons, N, is relatively small at d_1 and hence subject to high fluctuation, $\sim 1/\sqrt{N}$. As the cascade develops in the multiplier, it soon becomes statistically well defined since N increases rapidly with each subsequent dynode.

For completeness (11) and (13) must include an additional noise factor to allow for the multiplication noise.
They become:

$$S/N = (MT)^{\frac{1}{2}} \frac{I}{a} \qquad ...(14)$$

and

$$S/N = \frac{I_k}{(2 e I_k \Delta f)^{\frac{1}{2}}} \frac{I}{a} \qquad ...(15)$$

where, for a multiplier which obeys Poisson statistics

$$a = \left[\frac{\bar{\delta}}{\bar{\delta}-1} \right]^{\frac{1}{2}} > 1 \qquad ...(16)$$

This is a theoretical expression assuming Poisson statistics apply at each dynode of mean gain $\bar{\delta}$. However, in practice, the secondary emission process is poorly described by the simple statistical model assumed in (16). The measured output pulse height distribution for a photomultiplier excited by single photons (and hence single electrons at d_1) does not conform to the predictions of (16). The resolution is broader and there is an excess of small pulses in the distribution; see section 5.7. Examples of actual single electron distributions are shown in Figure 19.

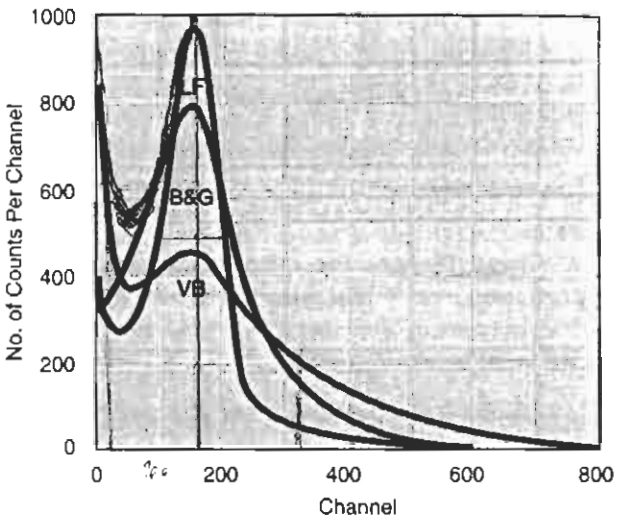

Figure 19

Single photoelectron pulse height spectra for various THORN EMI photomultipliers taken with a charge sensitive multi-channel analyser (equal area curves).

Noise factors can be deduced directly from any measured single electron distribution by numerical calculation of the variance, var(g), of the multiplier gain g. Var(g) is related to the standard deviation σ, by var(g) = σ². Thus:

$$a = \left[1 + \frac{var(g)}{\bar{g}^2} \right]^{\frac{1}{2}} = \left[\frac{\overline{g^2}}{\bar{g}^2} \right]^{\frac{1}{2}} \qquad ...(17)$$

Table 5.4

Calculated noise factors $\sigma(g)/\bar{g}$, $\overline{g^2}/\bar{g}^2$ and a by applying (17) to the curves of Figure 19. The entries for $\bar{\delta}_1$, in the penultimate column, are typical d_1 values for tubes of these types. The figures in the last column are calculated from (16).

Tube Type	σ(g)/ḡ	$\overline{g^2}/\bar{g}^2$	a	$\bar{\delta}_1$	$\sqrt{(\bar{\delta}_1/(\bar{\delta}_1-1))}$
V.B. 6097	0.760	1.58	1.26	10	1.05
L.F. 9814	0.52	1.27	1.13	16	1.03
B.G. 9924	0.57	1.32	1.15	10	1.05

The interpretation and practical use of these noise factors is straightforward. Referring to the 9814 photomultiplier, illustrated in Table 5.4, the S/N predicted by (11) and (13), which allows only for photocathode statistics, is further degraded by 1/1.13 or 0.89 by the action of the multiplier. A more detailed account of photomultiplier statistics and noise is given in the THORN EMI Technical Reprint Series [2].

The statistical considerations given in the above paragraphs account for the noise on the traces shown in Figure 15 and explain why a pulsed light source giving a constant mean number of photons per pulse leads to an ourput distribution with finite width. However, to explain why the measured rms noise is always greater than predicted by (14) or (15), we need to examine rhe contribution from dark current, and dark counts.

5.5 Dark Current and Dark Count

Outpur from a photomultiplier is obtained even in the absence of light input; this is referred to as **dark current** in dc applications and **dark count** in pulsed applications (also referred to as **background**).

If the dark current is observed on a chart recorder, a trace similar to Figure 20 will be obtained. There is variation around a mean value with large spikes superimposed at random times. Part of rhe fluctuation can be explained by conrributions from shot noise, but to account fully, it is necessary to examine the sources which contribute ro dark current. The dark current comprises a dc component (leakage current) plus a contribution derived from pulsed sources.

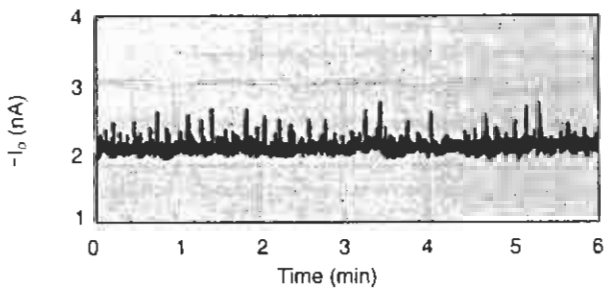

Figure 20

Dark current from a 9829 with a thin quartz window (at 2 × 10⁷ gain)

5.6 Dark Count Spectrum

The dark count spectrum depicted in Figure 21 shows a peak corresponding to the emission of single electrons from the cathode. Pulse height has been scaled in photoelectrons equivalent, using the peak as reference.

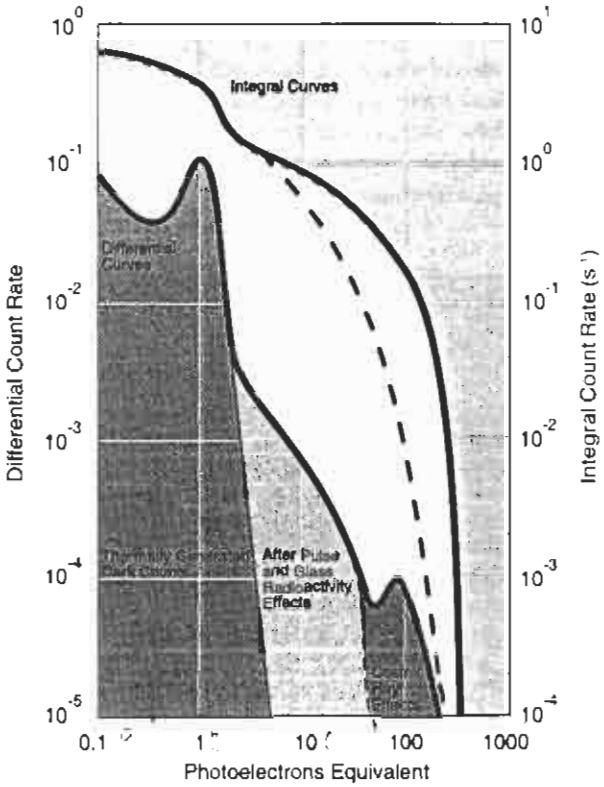

Figure 21

Illustrating dark counts at 20°C in a 9813Q as a function of pulse height. The differential curve normally obtained with a pulse height analyzer has also been integrated to provide count rate as a function of threshold. Data has been obtained at sea level (solid lines) and 30 merres underground (broken lines) to illustrate the contribution from cosmic radiation. Note the absence of the cosmic ray peak at about 100 photoelectrons equivalent, when underground.

The contribution i_q to dark current, from pulses in the spectrum of Figure 21, is given by integration of the curve where:

$$i_q = \int_0^\infty n(q)\, q\, dq \qquad \ldots(18)$$

where n(q) is the number of pulses/sec with charge q. If I' represents the contribution from leakage currenrs flowing into rhe anode, due to applied biassing voltages on the dynodes, then:

$$I_D = I' + i_q \qquad \ldots(19)$$

where I_D is the measured dark current. For a derailed explanarion of how I' is measured, the reader is referred to a rechnical publication on Photomultiplier Background [3]. Equation (19) provides an accurate description of dark current in phoromultipliers and correctly predicts the relationship between dark current and gain.

Figure 22 illustrates a number of points of practical significance. The dark current is dominared by the leakage component at low gain. I' varies linearly with applied voltage while i_q varies linearly with gain. This holds true until the onser of feedback at high gain where i_q starts to increase more steeply.

For dc measurements this suggests that for each tube there is a window of optimum performance for signal/background. In the photomultiplier characterised by Figure 22, this is at a gain of $2x10^7$. To find the optimum operating point it is sufficient to plot the ratio of signal (derived from a steady light source) to dark current, as a function of applied volts.

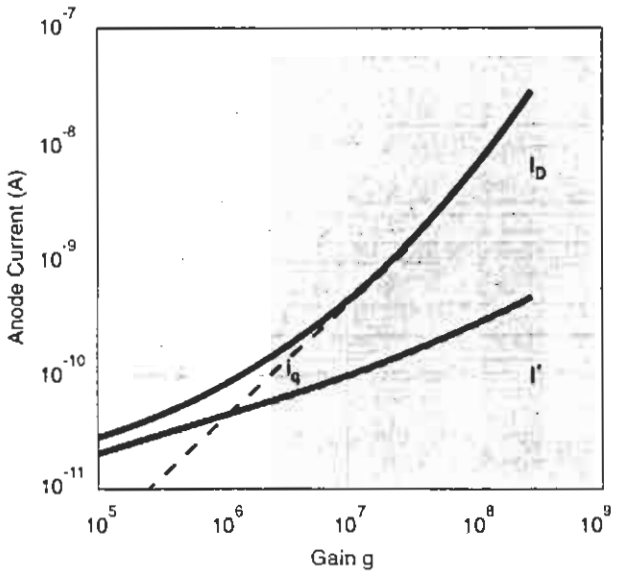

Figure 22

Dark current I_D comprises a leakage component I' and a contribution i_q from dark counts. Note how the measurements predict the correct magnitude of I_D and its dependence on multiplier gain, g.

To summarise; the output from a photomultiplier when viewing a steady light source shows fluctuations which can be explained by:

- contributions from statistical effects, referred to as noise-in-signal
- contributions from fluctuations in the dark counts

The dark current or dark count varies considerably even for photomultipliers of the same type. THORN EMI can provide photomultipliers selected for low dark current or dark count, to special order.

It should be noted that in dc measurements it is possible to back off the dark current but there is no way in which the fluctuations in dark current can be nullified. The fluctuations inherent in the signals shown in Figures 16 and 17 are due to statistical fluctuation in the number of photoelectrons in each pulse, the fluctuation in gain for each pulse, and a contribution from the dark count spectrum. It is important to understand the sources of background which contribute to Figure 21. Such knowledge helps explain why measured pulse height distriburions deviate from ideal.

5.7 Sources of Background

For the purpose of discussion it is convenient to divide the background pulse height distribution of Figure 21 into four regions: A, B, C and D.

Region A: Small pulses <0.5 photoelectrons equivalent. Small amplitude pulses occur in the signal and in the background. A proportion of these counts can be explained in terms of the statistical nature of photomultiplier gain. Contributions from thermionic electrons originating at the dynodes and secondaries generated from ion impact on the dynodes also contribute.

Region B: 0.5<B<2 photoelectrons equivalent. Contributions to this region are primarily caused by thermionic emission. However, on cooling the photocathode, a component attributed to natural radioactivity and other sources within the multiplier, remains.

Region C: 2<C<15 photoelectrons equivalent. Counts in region C are made up of afterpulses and from natural radioactivity in the window.

There is a finite probability that a signal or background pulse will be followed by a satellite or afterpulse. These are caused by ionisation of residual gases within the photomultiplier by the energetic electrons from the initial pulse. If the ion reaches the photocathode it is likely to cause a multielectron pulse; if intercepted by a dynode then a contribution to region A or B may result. Afterpulses are particularly undesirable in correlation studies or applications where temporal information is involved. The 9863 and 9130 ranges of photomultipliers provide performance with very low afterpulse rates.

Traces of naturally occurring ^{40}K, ^{238}U and ^{232}Th are present in all window material, although THORN EMI selects special glasses to minimise these contributions. The decay of these isotopes produces light by Cerenkov radiation and electrons by direct interaction with the photocathode. More detailed information on low background considerations is given in Section 5.9.

Region D: D>15 photoelectrons equivalent. These very large pulses are a direct consequence of the passage of cosmic rays (maitly muons and electrons) through the photomultiplier window. At sea-level this rare is about 15 per minute for a 51 mm diameter photomultiplier. Relativistic particles produce Cerenkov light emission in the windows. Since emission is biassed towards the UV, the quartz window variants give the largest pulse height. In each event, between 15 and 200 photoelectrons are produced depending on the window material, thickness and photocathode. In a typical event, the initial big pulse is followed by a series of single photoelectrons — up to 50 within a period of 100 µs.

5.8 Effect of Cooling

At room temperature the contribution from thermally generated electrons from the cathode dominates. The emission rate depends on the temperature, the photocathode type and the area. In addition to thermal electrons, pulses occur in this region from the sources previously discussed, such as cosmic radiation, natural radioactivity and afterpulses. However, these are unaffected by temperature. Figure 23 shows the effect of temperature on dark counts and the advantage of cooling in low level detection. For all cathodes, except the S1 type, there is little advantage in cooling below -25°C.

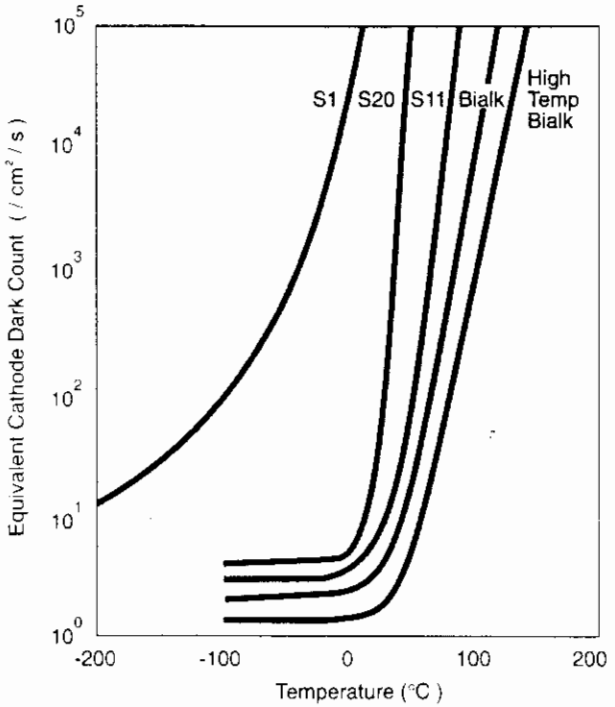

Figure 23

The dark counts from a photomultiplier as a function of temperature (above a threshold of 0.2 photoelectrons).

5.9 Low Background Glass

THORN EMI manufactures photomultipliers with low and ultra low levels of naturally occurring radio-isotopes. Their use is recommended in low background scintillation counting, with both organic and inorganic scintillators. In these applications the interaction of the isotope decay products with the scintillator itself results in large amplitude signals.

Absolute levels of radioisotopes, quoted in (ppm) or (ppb), are given in Table 5.9. These figures refer to levels of activity in the window only. Although other parts of the photomultiplier contribute, the window is the major source.

Total decays per minute, given in the penultimate column, refer to the total number of γ rays of all energies. Note that there is a spectrum of accompanying betas as well.

To give some perspective to the magnitude of this source of background, the counts in a 75 x 75 mm NaI(Tl) crystal are presented for a selection of glasses offered by THORN EMI. The last column in 5.9 gives an indication of the contribution to the count rate of a 75 x 75 mm NaI(Tl) crystal in contact with the stated window material. The actual count rate in any particular arrangement depends quite critically on where the lower energy threshold is set, so these figures should be regarded as order of magnitude only.

Table 5.9

Background levels in photomultiplier windows. Decays per minute refer to a 50 mm diameter window of weight 30 g.

Material	K (ppm)	Th (ppb)	U (ppb)	Total Decays /min	Contribution Counts /min
Standard Borosilicate	<60,000	<1000	<1000	<400	<100
Low Background	300	250	100	25	5
Ultra Low Background	60	20	10	5	1
Quartz	<5	<5	<5	<0.3	<0.1

5.10 Photomultiplier Stability

The overall sensitivity of the photomultiplier is known to vary:

- with operating time while maintaining constant illumination, applied voltage and ambient conditions.
- on switching the output current, after removing and reapplying either the light input or overall voltage.
- with change in ambient temperature and external electromagnetic fields. These environmental effects are discussed in Section 6.

Stability

The action of drawing anode current alters the secondary emission coefficient of the dynodes, in particular the later stages where current densities are highest. The slow variation of anode current with operating time is usually termed 'drift' and its magnitude depends on the dynode surface (Figure 24) and on the mean anode current (Figure 25).

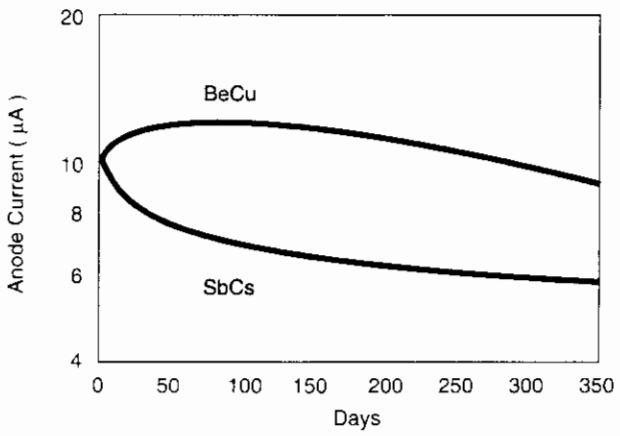

Figure 24

Sample stability curves for photomultipliers illustrating the different performance with BeCu and SbCs dynodes. The stability of individual tubes varies within the same type.

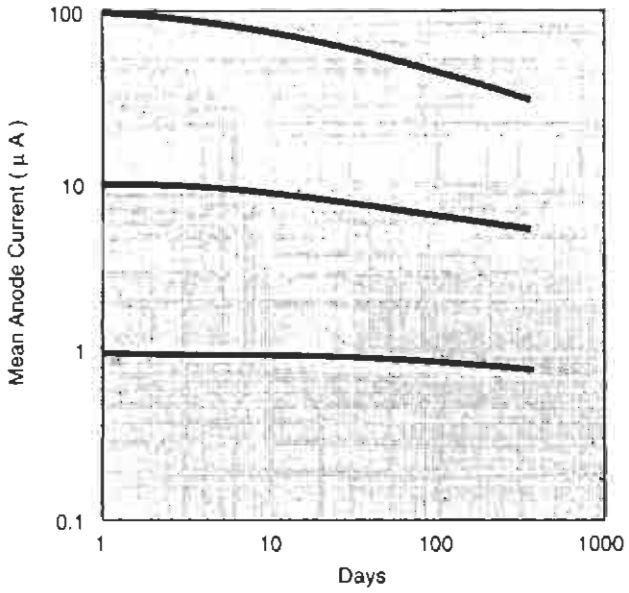

Figure 25

Illustrating long term stability (1 year) for SbCs dynodes as a function of mean anode current, under conditions of constant applied voltage and illumination.

The change in multiplier gain is not necessarily permanent; if the photomultiplier is switched off it will slowly recover its initial performance. Where srability is of prime importance, the recommendation is to maintain the anode current below 1 μA.

Hysteresis

When a light source of constant intensity is interrupted and rhen re-applied, the photomultiplier may not immediately recover its previous anode current level. The effect shown in Figure 26 is attributed to charging effecrs within the photomultiplier which temporarily alter the photomultiplier gain.

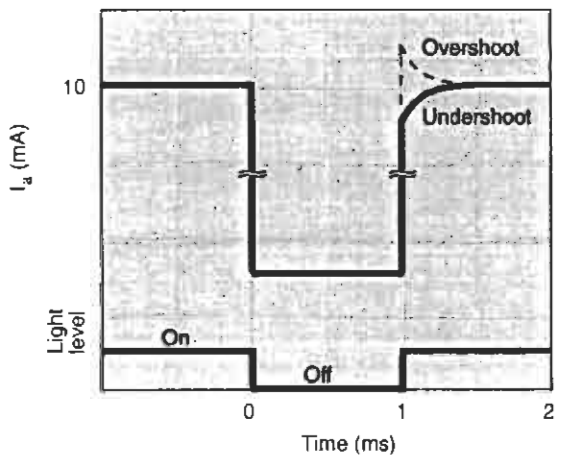

Figure 26 a)

Sample curves illustrating hysteresis effects after switching light input ON/OFF/ON. Photomultiplier type 9106 operated at 10^4 gain. The overshoot is of the order of 0.5%.

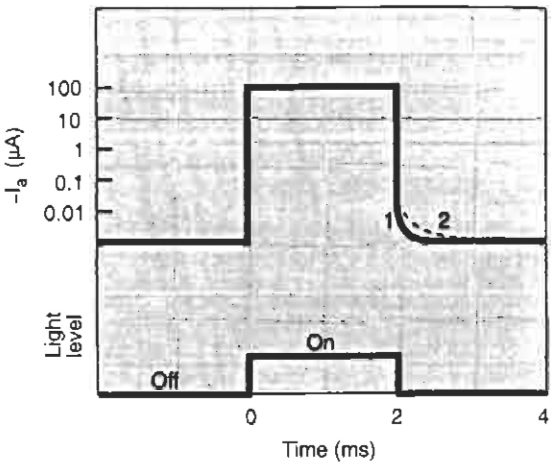

Figure 26 b)

Sample curve illustrating memory effects after switching light input OFF/ON/OFF.

1. 9781 anti-hysteresis design.

2. 9781 without anti-hysteresis design.

A similar effect may occur when the overall voltage is removed and then re-applied. The effect is more pronounced if the illumination is maintained during the off period. The magnitude of these hysteresis effects and the recovery time are determined by the mean current, gain, dynode surface, and the multiplier structure. Linear focused variants, such as the 9102, and side window types have excellent recovery characteristics.

Rate Effect

In pulsed applications there is a hysteresis effect which produces a change in pulse height with count rate. It is not directly the count rate which causes the effect but the related changing anode current. Such an effect can be caused by poor voltage divider design but for the present we refer to an intrinsic dynode gain variation only. In NaI(Tl) applications, a standard test is to change the position of a ^{137}Cs source on the axis of the scintillator producing at first pulses at a rate of 1000 s^{-1}, then pulses at 10,000 s^{-1} and observing the mean pulse height in each case. For the test to have any meaning, the gain must be specified. In high energy physics applications count rate may increase to many MHz for short time durations.

The cause of rate effect is not fully understood but what is well established is that THORN EMI SbCs dynodes offer far superior performance to BeCu dynodes. In photomultipliers with BeCu dynodes there will be gain changes at the 1% level for anode currents in excess of 1 μA. With SbCs dynodes the level of performance is a factor of ten better under similar conditions. Where rate effect is critical, selection for this parameter is recommended.

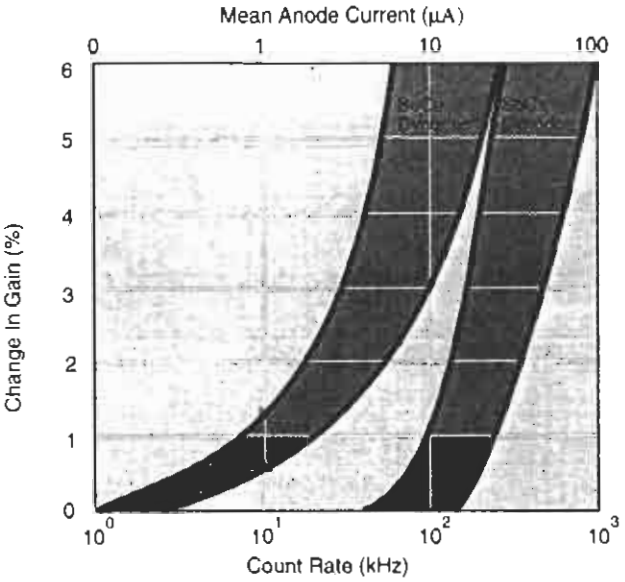

Figure 27

The change in gain with increasing count rate is known as the rate effect. The gain change is related directly to the mean anode current, which in turn is a function of count rate. The rate effect is independent of gain. The shaded regions indicate the spread in this parameter from tube to tube of the same type.

5.11 Pulse Height Resolution

Pulse height resolution is an important, practical measure of the ability of a photomultiplier to reveal structure in spectral measurements. The source of the spectrum of pulse heights may be a NaI(Tl) crystal excited by a mixture of isotopes, or some other light emitting process where peaks in the distribution have some physical significance. In both cases the resolution, R, is by definition:

$$R = \frac{fwhm}{peak\ position} \times 100\ \% \qquad ...(20)$$

where fwhm is the full width at half maximum height

For a Gaussian distribution, the relationship between standard deviation, σ, and resolution is:

$$Resolution = 2.36\,\sigma \qquad ...(21)$$

where σ is expressed as %

Equation 21 can be used with confidence for most practical distributions. A spectrum measured with a 9266B coupled to a Ø 44 x 44 mm NaI(Tl) crystal is shown in 28(a). The peak in the distribution corresponds to the capture of the entire energy of the ^{137}Cs monoenergetic gamma-ray and is known as the photopeak.

Applying the definition of (20) to this distribution gives a resolution of 6.9%. The complete capture of a ^{137}Cs gamma-ray in a NaI(Tl)/photomultiplier combination corresponds to about 5000 photoelectrons from the photocathode (a useful figure to remember is ~8 photoelectrons/keV for a 2" x 2" crystal). From the statistical arguments culminating in (14), taking the mean number of photoelectrons as ~5000, the expected resolution should be about half that measured. The explanation for this discrepancy lies in the intrinsic resolution associated with NaI(Tl) crystals[2].

Figure 28(b) illustrates an application at the low energy end of the X-ray scale. The 5.9 keV X-ray from ^{55}Fe corresponds to only ~80 photoelectrons and in this case the width of the distribution is reasonably well described by (14). A low energy tail is always present in ^{55}Fe spectra. This stems from contributions originating in regions C and D in the background spectra.

The photomultiplier used to obtain the spectrum in Figure 28(b) included a low background window and was selected for low counts. With an unselected tube, the dark signal can encroach to 1-2 keV and affect the resolution.

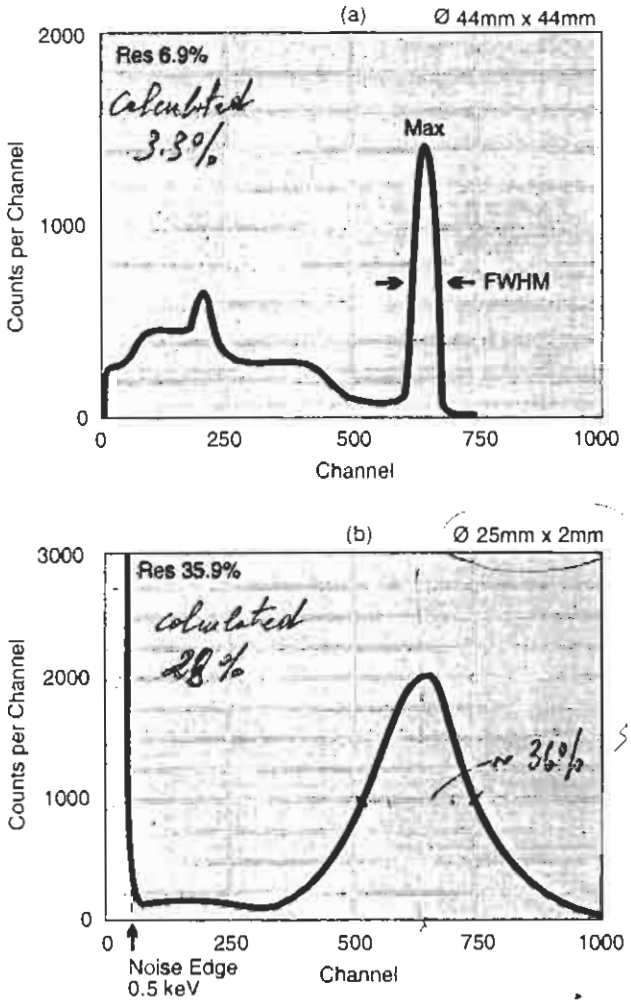

Figure 28

Typical spectra from NaI(Tl) scintillators, optically coupled to a 9266 photomultiplier responding to radioactive decay from (a) ^{137}Cs, and (b) ^{55}Fe.

Table 5.11 gives NaI(Tl) resolution figures for common isotopes. It is important to appreciate that resolution is always sensitive to the quality of crystal used.

Table 5.11

Typical pulse height resolution for photomultipliers optically coupled to THORN EMI, NaI(Tl) reference, crystals. The yield in photoelectrons/keV (pe/keV) is given in the second row.

Isotope	^{55}Fe	^{129}I	^{57}Co	^{137}Cs	^{60}Co
Energy (keV)	6	30	122	662	1332
pe/keV	12	8	8	8	6
Crystal mm (dxh)	20×3	25×25	44×44	50×50	75×75
Resolution (%)	32-40	25-35	8.5-10	6.8-7.4	10-15*

* It is standard practice to quote ^{60}Co performance in terms of the peak-to-valley ratio referred to 1.332 MeV, rather than in terms of resolution.

6 Environmental Effects

Photomultiplier operation is sensitive to environmenral conditions. Precautions can be taken to limit the environmental effects but often more can be gained by the correct choice of tube for the particular application.

6.1 Temperature

Dark Current and Dark Count

Photomultiplier dark current and dark count rate are critically dependent on temperature. This is illustrated in Figure 23 where for most cathode types there is a doubling in dark current every 5°C rise above room temperature. Dark current varies considerably even for photomultipliers of the same type. THORN EMI can provide photomultipliers selected for low dark current or dark count rate. Detailed specifications for dark current and dark count rate are given for each tube type in the Photomultiplier Characteristics section of this catalogue.

Overall Sensitivity

The overall sensitivity varies with temperarure because of the combined effects of cathode sensitivity and multiplier gain changes.

The electron multiplier gain change is approximately −0.2 %/°C for both BeCu and SbCs dynodes.

The change in photocathode sensitivity wirh temperature depends on the photocathode type and the wavelength of incident light as illustrated in Figure 29. Note how the variation is greatest at the long wavelength limits of sensitivity. The loss in red sensitivity should be noted whenever cooling is employed to reduce dark counts. The temperature coefficient of rhe photomultiplier is the combinarion of the change in photocathode sensitivity and electron multiplier gain, e.g. −0.3 %/°C for the 9954 at 400 nm.

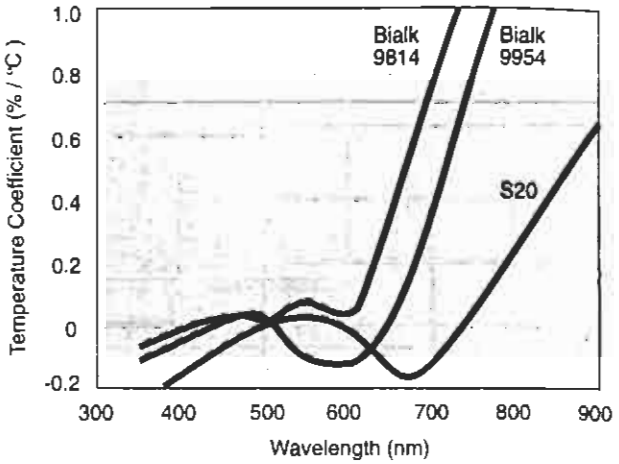

Figure 29

Temperature coefficient of photocathode sensitivity for various THORN EMI photomultipliers.

The resistivity of the photocathode layer increases with decreasing temperature. Therefore below room temperature the maximum current that can be drawn from the photocathode, if non-linear operation is to be avoided, is less than the value quoted in Table 5.3(a). Maximum currents must be scaled by a factor of 2 per 5°C temperature drop below 20°C.

6.2 External Magnetic Fields

An external magnetic field causes photoelectrons and secondary electrons to deviate from their normal trajectories. The effect is critically dependent on electron optical design and multiplier structure, the focused structures being most susceptible. Both photoelectron collection efficiency and electron multiplier gain, g, are affected, giving a combined effect on the overall gain G, as illustrated in Figure. 30.

Use of a mu-metal shield is recommended to minimise the effect and in the best designs extends from the rear of rhe photomulriplier to a disrance half of the diameter beyond the photocathode.

THORN EMI offers integral mu-metal shields for end window photomultipliers up to 52 mm diameter. Figure 31 shows the construction of an integral shield; the mu-metal is wrapped around the graphite coated envelope and electrically protected by an insulating sleeve. The relative output of the photomultiplier is shown in Figure 32 as a funcrion of external magnetic field with an integral shield. Further details on this technique and the benefits it offers are contained in the THORN EMI reprint RP 084[4].

6.3 External Electric Fields

Phoromultiplier stability and lifetime is strongly influenced by electric fields. It is importanr to distinguish between truly external and internal electric fields. By internal is meant the electrical field generated in the glass envelope and immediate surroundings of the photomultiplier by the application of high voltage. This electric field that is more often responsible for

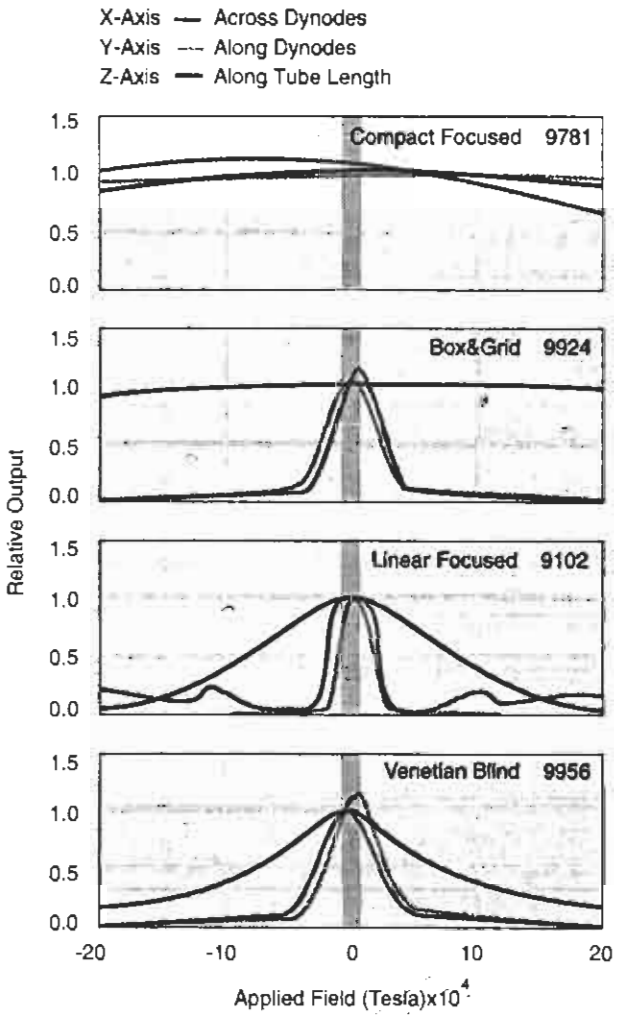

Figure 30

Relative output as a function of external magnetic field. (For photomultipliers operated at normal gain).

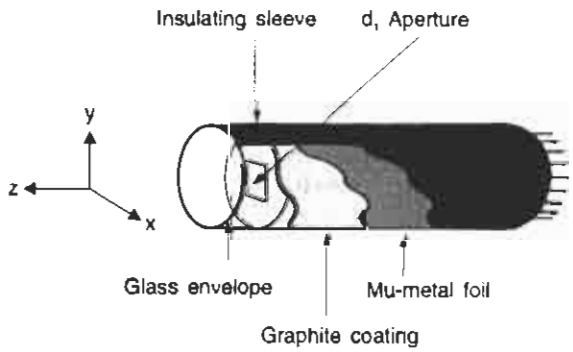

Figure 31

Cut away section illustrating the construction of the integral mu-metal shield. The co-ordinate axes adopted for the photomultiplier are also shown.

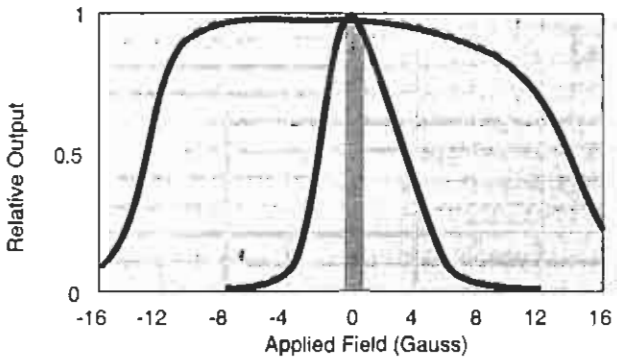

Figure 32

Demonstrating how a wrapped mu-metal shield reduces the sensitivity of a 9106 photomultiplier to external magnetic fields. Solid line: unshielded; grey line: wrapped shield; shaded region: earth's field. Field aligned along length of first dynode, Y axis.

erratic and unstable photomultiplier behaviour than any other source. The photocathode region is the most sensitive part of the photomultiplier to field gradients.

Gain stability and dark counts are affected by field gradients in the vicinity of the photocathode. This is illustrated in Figure 33 where dark counts are recorded as a function of envelope potential. In this investigation, a cylindrical screen covering the envelope, but leaving the window free, was varied in potential using a separate power supply. The effect on performance is dramatic and represents typical behaviour when photomultipliers are operated under these conditions.

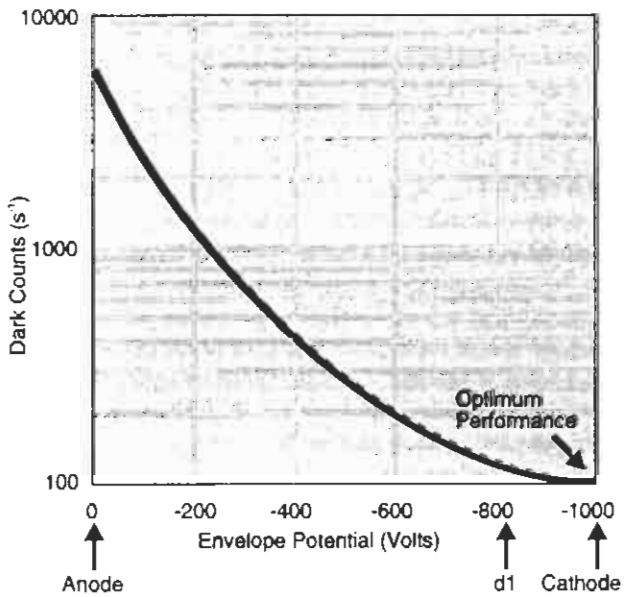

Figure 33

Effect of envelope potential on the dark counts of a 9924 photomultiplier. Best performance is obtained when the envelope is maintained at cathode potential.

The use of positive high voltage dictates that the cathode is at ground potential. If associated housings, shielding and material in contact with the window (for example a NaI(Tl) crystal) are all maintained at ground potential then there will be no field gradients and stable performance is assured. Positive high voltage is always the preferred mode of photomultiplier operation where the anode is ac coupled.

Certain photomultiplier applications demand the use of negative high voltage (where the anode is directly coupled to external circuitry). Optimum and stable performance can be obtained provided precautions are taken to eliminate electric field gradients in the vicinity of the window. Figure 34 illustrates the precautions to be taken when a NaI(Tl) crystal is coupled to a photomultiplier. **It is not acceptable practice to ground the can of the crystal. Instead it must be maintained at cathode potential, and, in addition, insulated from the surroundings.**

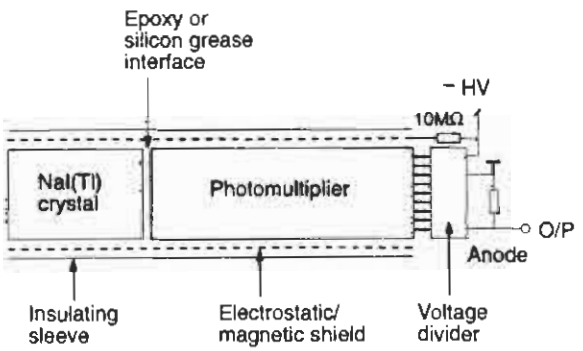

Figure 34

Stable performance with negative high voltage is achieved by eliminating potential gradients in the vicinity of the photocathode. The electrostatic shielding and the can of the crystal are both maintained at cathode potential by this arrangement.

Important

Any conductor in contact with the window or envelope of the photomultiplier must be connected to cathode potential. When the photomultiplier is operated at cathode negative with respect to ground, a 10 MΩ safety resistor between -HV and the shield is advised. Only very good insulators, e.g. PTFE, should be brought into direct contact with the photomultiplier window. All too often, unstable output, high dark current and reduced photomultiplier lifetime can be traced to a ground contact on the photomultiplier window (or envelope) when the photomultiplier is operated with cathode negative with respect to ground. For similar reasons the casing of NaI(Tl) crystals must be maintained at cathode potential.

RFI shielded ambient and cooled housings, available from THORN EMI, have been designed for use with positive or negative high voltage by observing the precautions outlined above.

THORN EMI can also provide a graphite coating on the envelope of the photomultiplier, with the graphite connected directly to the cathode pin. An insulating sleeve covers the graphite for safety reasons, adding approximately 0.8 mm to the published photomultiplier diameter. This option is especially recommended in low light level applications.

6.4 Effect of Ionising Radiation

As discussed in Section 5.7 ionising radiation causes electron emission in the photomultiplier. At high energies it causes 'browning' of the glass window and envelope affecting transmission of light to the photocathode. The amount of discolouration depends on the exposure and on the type of glass; a quartz (fused silica) window is least affected.

6.5 Shock and Vibration

Photomultipliers will withstand the demands of portable instrumentation and everyday handling. There are, however, levels of shock and vibration which will cause mechanical failure or impair electrical performance.

Excessive shock can give rise to mechanical failure should any support or electrical connection fracture. Excessive vibration gives rise to mechanical failure of the envelope or of the internal structure. In addition loose material may be produced which can accumulate and cause internal short circuits.

Shock and vibration can manifest itself at the anode as microphony — caused by changes in electrode capacitance from movement of electrodes. In addition, where ac coupling is used, the coupling capacitor itself may be microphonic. The use of charge sensitive amplifiers minimises these effects. Mu-metal shields are recommended to eliminate the effects of changing magnetic fields. When operated at negative high voltage, external insulators or potting materials in contact with the envelope may break-down electrically or produce light. The method of mounting a photomultiplier is critical: encapsulation can be designed to damp external shock and vibration. Flexible potting materials applied over the full length of the photomultiplier are generally recommended for radial support. Axial load is recommended to prevent movement of the window with respect to the housing.

Glass and quartz photomultipliers can be specially manufactured to meet severe operating conditions experienced for example in military, oil well logging and space launch applications. THORN EMI will design, qualify, manufacture and test devices to specific project requirements. After qualification it is normal practice to test all project devices at an acceptance level, which is half of the qualification level.

THORN EMI has extensive environmental test facilities including sinusoidal and random vibration, shock, thermal and vacuum test. Representative shock and vibration tests are shown in Table 6.5 while Figure 35 illustrates power spectral density curves for random vibration. The frequency range, acceleration values and test duration are agreed with each customer.

Table 6.5

Shock and vibration limits for glass and metal ceramic photomultipliers. These limits apply for all orientations, with the photomultiplier non operational. The frequency profile shown in Figure 35 applies to random vibration.

Parameter	Test	Glass/Quartz Types	Metal Ceramic Types
Shock (½ sine)	ĝ	30 ĝ	250 ĝ
	Duration	11 ms	2 ms
	Shocks/axis	3	30
Sinusoidal Vibration	Frequency	10-32 Hz	10-32 Hz
	Amplitude (p-p)	10 mm	10 mm
	Frequency	32-2000 Hz	32-2000 Hz
	ĝ	20 ĝ	30 ĝ
	Sweep rate	1 octave/min	2 octaves/min
Random Vibration	Maximum	0.6 g^2/Hz	2 g^2/Hz
	Composite	20g rms	36 g rms
	Duration/axis	2 mins	10 mins

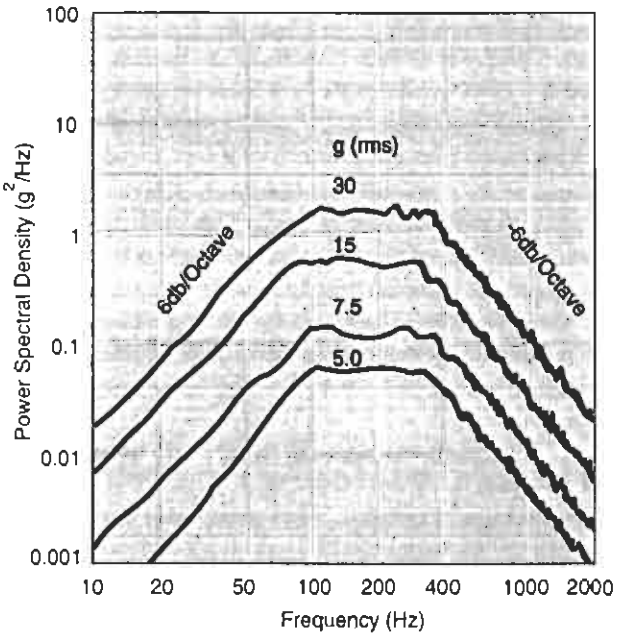

Figure 35

Standard random vibration power spectral density profiles used by THORN EMI. The square root of the area under each curve is related to g(rms).

6.6 Exposure to Daylight

The photomultiplier is an extremely sensitive light detector and should not be operated under daylight or room lighting levels. Even when non-operational, exposure to daylight or normal lighting levels causes photocathode excitation, especially under UV illumination. Although this does not damage the tube, it causes an increased dark current (count) level. Initially this may be several orders of magnitude higher than the final dark current value. The effect is particularly pronounced in photomultipliers with quartz windows. Although the photomultiplier can be used immediately after exposure without any effect on overall sensitivity, the dark current will not settle to its ultimate value for many hours. Figure 36 illustrates the typical dark current decay of a 9829Q. For these reasons it is recommended that tubes are not exposed to daylight or fluorescent room lights but are loaded into instruments under subdued lighting conditions.

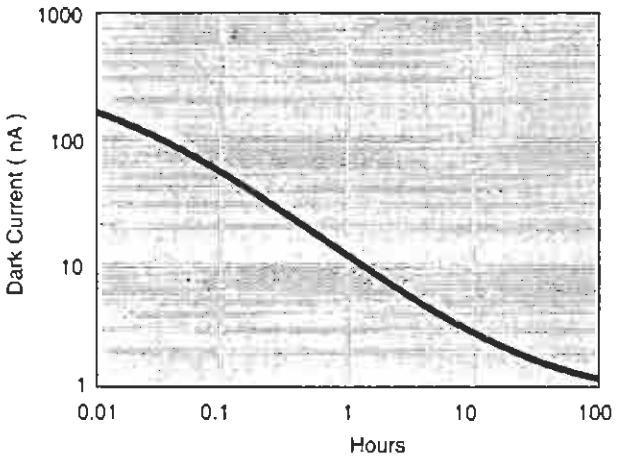

Figure 36

Typical dark current decay of 9829Q after exposure to daylight for 1 hour (non-operating).

6.7 Helium

Helium is able to permeate glass, especially quartz (fused silica). While chemically inert, the increase in gas pressure within the photomultiplier results in an increase in afterpulse rate. If the pressure exceeds 10^{-2} torr, electrical breakdown becomes likely and the photomultiplier becomes inoperable. **For this reason storage or operation in helium-enriched environments must be avoided.**

7 Choice of Photomultiplier

At first sight this appears to be a formidable task because of the number of variants offered by THORN EMI. However, the choice is rapidly reduced to within a few, or just one device, when external factors and performance characteristics of particular photomultipliers are considered. External factors such as the area over which the light extends and physical constraints on overall dimensions usually play an important role in selection. Performance measurements requirements such as:

- spectral response
- gain
- dark current
- linearity
- speed of response

invariably reduce the choice to within a few types.

7.1 End Window or Side Window

The overall performance offered by the two types usually favours the selection of the end window form. In end window tubes there is a wide choice of active areas, photocathode types and window geometry. Gathering the maximum light flux on to the photocathode from remote, diffuse and directly coupled light sources is best with an end window. The side window types are recommended when space is limited or when light levels are very high.

7.2 Spectral Response

The most suitable photocathode type is the one that has the maximum quantum efficiency over the wavelength range emitted by the light source. At low light levels the signal to background ratio may be more important. At high light levels consideration should be given to the maximum cathode current allowed. This is discussed in detail in Section 5.3. The choice of window is important when the light source to be measured emits in the UV. Transmission curves given in Section 3.2 should be consulted. In the detection of ionising radiation using a scintillaror, there is a contribution to background count rate from the naturally occurring isotopes in the photomultiplier window. When this is critical, it is advisable to discuss your particular requirements with THORN EMI.

7.3 Electron Multiplier Structure

The choice is often restricted by the diameter of the phoromultiplier; the widest variety of multipliers is available in 52 mm diameter tubes.

The linear focused structure is recommended in pulsed light applications for fastest time response, for best linearity and for highest available multiplier gain.

The circular focused structure is the most compact design with good magnetic immunity, good timing and good linearity but is limited in the number of stages available.

The venetian blind is an excellent general purpose structure with a wide choice in the number of stages.

The box and grid structure is most commonly used in 30 mm diameter photomultipliers and is suited to a variety of applications from high light levels down to the photon counting region.

7.4 Number of Dynodes

It is important to choose a photomultiplier with the correct number of stages. When too many stages are chosen to provide the required gain, the electrical performance is degraded. This is a consequence of low inter-electrode voltages, causing poor linearity and timing. If too few stages are chosen, there may be insufficient gain available within the constrainrs of the maximum allowed operating voltage. Operation beyond the maximum overall sensitivity will result in excessive dark current, breakdown and short lifetime.

For low light intensities, down to photon counting levels, 11 to 14 stages will be required. For high light levels, 6 and 9 stages are usually sufficient (high light levels are those that can be seen by the human eye). An aid to selecting the right number of stages is presented in Table 7.4.

Table 7.4

Relationship between light level and number of dynodes.

Light level	Photocurrent	Gain Required	No.of Dynodes
Low	<10pA	$>10^5$	14 - 12
Intermediate	10pA - 1nA	10^4 - 10^6	11 - 9
High	>1nA	$<10^4$	8 - 6

7.5 SbCs or BeCu Dynode Surface

At any applied voltage SbCs dynodes have higher gain than BeCu ones but this is not always an advantage. Since the time response depends on applied voltage, BeCu is recommended for time-critical pulsed light applications. In addition, it provides better pulsed current linearity.

SbCs requires lower operating voltages. It also has better hysteresis and rate effect performance due to its low surface resistivity, enabling it to settle quickly between changing light levels. Consequently it is the best choice in optically chopped light applications such as colour film scanning. Further details are given in Sections 4.3 and 5.

7.6 Electrical Performance

As explained in Section 5, various limitations apply in photomultiplier performance which may further influence the choice of photocathode, multiplier structure and number of dynodes. Reference should be made to this Section before making the final choice.

Having chosen the most suitable photomultiplier, it is recommended that a prototype of the optical detection system is built. It is important to confirm the mean cathode current, the mean and peak anode current and the range of operating voltages. 'Order of magnitude calculations' are sufficient for this purpose. It is often found that the light levels are either much higher or much lower than expected and re-selection of the most suitable photomultiplier may be necessary.

Manufacturers are continually upgrading equipment performance, which may place additional demands on the photomultiplier. Engineers making changes which affect the operating voltages or the currents flowing in the photomultiplier should always re-confirm that the phoromultiplier remains within its performance limits. When re-design takes place, it is advisable to contact THORN EMI to keep up to date with the latest products.

8 Voltage Dividers

A series of voltages is applied to the photomultiplier to accelerate and focus photoelectrons on to d1, to accelerate and focus the secondary electrons between successive dynodes and to collect the secondaries from the last dynode at the anode. It is common practice to derive the voltages from a single supply using a resistive divider network.

Voltage divider design is critical to achieving optimum performance from a phoromultiplier. An outline of design considerations is given in this section but for a detailed account, the reader is referred to *'Voltage Divider Design'* RP069[6].
All phoromultipliers will operate with the linear divider, shown in Figure 37, although not necessarily with ideal performance.
For example, if linearity and timing are of prime importance, it will be necessary to modify the basic configuration of Figure 37.
Voltage dividers actually used by THORN EMI for testing purposes are listed on page 62 of this catalogue.

8.1 dc Applications

Direct current applications require negative high voltage applied at the cathode, leaving the anode at ground potential for ease of interfacing. The choice of R in Figure 37 is governed by rhe maximum anode currenr I_a(max) the application demands, subject to I_a(max) always <100 μA. R should be chosen to satisfy the relationship I_a(max)<0.01 I_{HV}, where I_{HV} is the divider current. This will ensure rhat gain linearity is preserved up to anode currents of I_a(max). Once I_a(max) exceeds one tenth I_{HV}, serious deviation from linearity will become apparent.

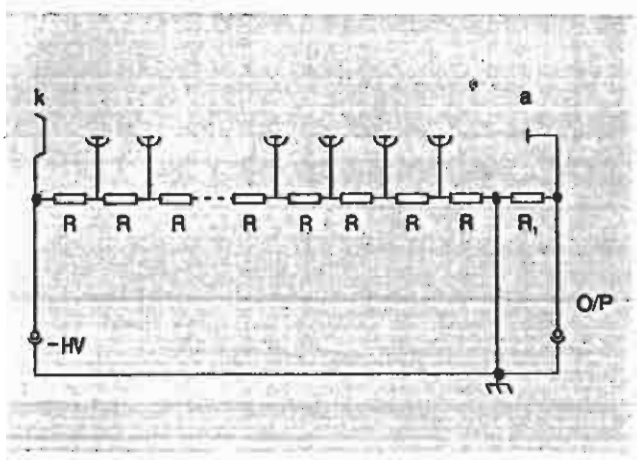

Figure 37

The linear voltage divider for dc applications. R may be in the range 10kΩ-10MΩ. R_1=10MΩ is a safety resistor, which prevents the anode floating to d_n potential when the external load is removed.

8.2 Pulsed Applications

Some photomultipliers are capable of handling peak currenrs of the order of 200 mA. To achieve this level of performance requires a divider that differs from that in Figure 37 in two important respects:

1) the potentials applied to the last few stages must be increased to overcome space charge effects;
2) capacitors are added to supply the charge pulse.

With NaI(Tl) applications it is common to use pusitive high voltage with the cathode at ground potential. The coupling capacitor, C, shown in Figure 38, isolates rhe dc potential at the anode from the measuring electronics. In high energy physics applications it is usual to couple the anode directly to external electronics to avoid overshoor.

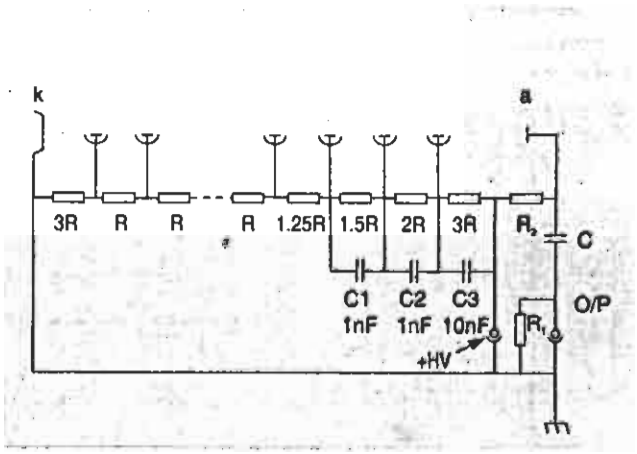

Figure 38

A tapered divider suitable for pulse applications. In this example, positive high voltage is used. R_2 is the load resistor, 10kΩ-1MΩ. R_1=10MΩ safety resistor.

As with the linear voltage divider of Figure 37, R is chosen to satisfy:

$$I_{HV} > 100\,\bar{I}_a \qquad ...(22)$$

Where $\bar{I}_a$ is the mean anode current.

The degree of taper on the last few stages of the divider depends on the tube type and on the level of performance required. As a guide use the recommendations on page 62.

The size of decoupling capacitors can be calculated from the basic relationship for a capacitor: Q = CV. It is sufficienr to demand that the interdynode voltage remains constant to ~0.1%, that is ΔV/V ≤0.001, while peak charge ΔQ is drawn.
If C is chosen to satisfy:

$$C > \frac{\Delta Q / V}{\Delta V / V} \qquad ...(23)$$

the divider will cope wirh short bursts of pulses of variable magnitude. It is important to appreciate that decoupling capacitors only cover short bursts of pulses. A sustained high count rate leads to a high mean anode current $\bar{I}_a$ and there is the possibility thar the relationship (22) will be violated.

A resistive divider poses a power dissipation problem, if properly designed in accordance with (22), for high count rares. Practical dividers, ideal for high counr rates, either incorporate zener diodes or transistors in the final stages. These provide the required level of performance without the need to draw excessive divider current. This is a specialised subjecr on which THORN EMI will be pleased to advise.

References available on request:

1) Gating of Photomultipliers (RP C61).
2) Monte Carlo Simulation of Photomultiplier Resolution (RP C80).
3) An Investigation of Photomultiplier Background (RP 075).
4) Integral mu-metal Shields (RP C84).
5) Metal Ceramic Photomultipliers (RP 079).
6) Voltage Divider Design (RPC69).

This selection guide cross references photomultiplier types, performance attributes and applications. Section 5, **Limits on Performance**, and section 7, **Choice of Photomultiplier**, in the introductory section of this catalogue should be consulted as part of the selection process.

	Characteristics						Features																	Applications												
Type	Spectral response	Diameter mm	CsSb	BeCu	Stages	Multiplier	Low background window	Quartz window for UV (option)	MgF_2 window for VUV	High gain	Extended linearity	Single electron resolution	NaI (Tl) resolution	Low rate effect	High speed, large bandwidth	High temperature	Rugged	Compact	Low dark current/count	Gateable	Housing available	Low cost voltage divider	Magnetically screened option	Gamma spectroscopy/counting	Photon counting	Emission spectroscopy	Absorption spectroscopy	Pollution monitoring	Fluorescence spectrophotometry	Colour scanner	Bio/Chemiluminescence	Radio immuno assay	Severe environment	Liquid scintillation counting	High light level	High energy physics, Astrophysics
6097	S11	52	●		11	VB		●		●				●							●															
9078	Bialk	19	●		10	LF	●	●			●	●	●	●	●			●	●		●		●	●		●				●		●				●
9079	S20	19	●		10	LF	●	●			●	●		●	●			●			●		●			●		●	●	●						
9082	Bialk	19		●	10	LF	●	●			●	●	●		●			●	●		●		●	●		●		●	●	●						●
9102	Bialk	38	●		10	LF	●	●			●	●	●	●	●			●	●		●		●	●	●	●										
9108	RbCs.	30	●		7	LF	●	●			●			●	●			●	●		●		●							●					●	
9110	H Bialk	25		●	10	CF	●						●		●	●	●	●	●				●	●									●			
9111	Bialk	25	●		10	CF	●	●					●	●	●			●	●				●	●			●	●								
9112	RbCs	25	●		10	CF	●	●					●	●	●			●					●	●			●	●								
9113	S20	25	●		10	CF	●	●						●	●			●					●		●		●	●								
9124	RbCs	30	●		11	LF	●	●		●	●	●	●	●	●						●	●	●		●	●	●		●		●					
9125	Bialk	30	●		11	LF	●	●		●	●	●	●	●	●				●		●	●	●	●	●	●	●		●		●	●				
9128	Bialk	30		●	11	LF	●	●		●	●	●			●				●		●	●	●													●
9129	S20	30		●	11	LF	●	●		●	●	●			●						●	●	●			●	●	●								
9130	S20	30		●	11	LF	●	●		●	●				●				●		●	●	●		●	●										
9131	Bialk	30		●	11	LF	●	●		●	●				●				●		●	●	●		●	●										
9132	Bialk	30		●	11	LF	●	●		●	●	●			●				●			●	●											●		
9133	RbCs	25	●		9	LF	●	●			●		●	●	●			●	●				●	●												
9134	Bialk	30	●		9	LF	●	●			●			●	●			●	●				●							●					●	
9135	RbCs	25	●		10	LF	●	●			●		●	●	●			●					●	●												●
9136	S20	30	●		11	LF	●	●		●	●	●		●	●			●			●	●	●		●	●	●		●							
9202	S20	52	●		11	LF		●		●	●	●		●	●						●		●		●	●		●		●						
9203	S20	52	●		11	LF		●		●	●	●		●	●						●		●		●	●		●								
9205	Bialk	52	●		10	LF	●	●			●	●	●	●	●						●		●	●												
9206	S1	52		●	10	LF	●	●			●				●						●		●			●										
9207	H Bialk	52		●	13	LF	●			●	●		●		●	●	●		●		●			●									●			
9214	Bialk	52	●		12	LF	●	●		●	●	●		●	●					●	●	●	●	●	●											●
9223	H Bialk	32		●	12	VB	●						●			●	●		●					●									●			
9224	H Bialk	26		●	12	VB	●						●			●	●	●	●					●									●			
9228	H Bialk	51		●	14	VB	●			●			●			●	●		●					●									●			
9235	Bialk	52	●		13	LF	●	●		●	●	●	●	●	●				●		●		●		●									●		
9236	Bialk	60	●		10	LF	●	●			●	●	●	●	●				●					●												●
9250	Bialk	52	●		10	LF	●	●			●	●	●	●	●				●		●		●	●										●		
9256	RbCs	52	●		10	LF	●	●			●	●	●	●	●						●		●	●							●					
9257	RbCs	52		●	10	LF	●	●			●	●	●		●						●		●	●							●					
9265	Bialk	78	●		9	LF	●	●			●	●	●	●					●					●												
9266	Bialk	52	●		10	LF	●	●			●	●	●	●	●				●		●		●	●												
9301	S20	78	●		9	LF	●	●			●	●		●										●												
9330	Bialk	130	●		11	LF	●			●	●	●	●	●										●												
9350	Bialk	200	●		14	LF	●			●	●	●		●	●																					●
9352	Bialk	200		●	6	LF	●				●				●				●																	●
9353	Bialk	200	●		12	LF	●			●	●	●		●	●																					●
9370	Bialk	130		●	12	LF	●			●	●	●			●				●																	●
9390	Bialk	130	●		10	LF	●	●			●	●	●	●										●												●
9402	CsTe	30	●		11	LF		●	●	●	●			●	●				●		●	●	●			●										●
9403	CsI	30	●		11	LF		●	●	●	●			●	●				●		●	●	●			●										●
9405	RbTe	30	●		11	LF		●	●	●	●			●	●				●		●	●	●			●										●
9422	CsTe	52		●	14	LF		●	●	●	●				●				●	●	●	●	●													●

TUBE VARIANTS – Suffix Designations

In addition to the basic type number, a letter suffix is used to denote electrical characteristics or mechanical features. Special selection is indicated by a number suffix.

- A Selection to one-off requirement. Specification details must accompany the order.
- B Standard published specification.
- E Electrostatic shielding protected by a black plastic insulating sleeve.
- FL Photomultiplier supplied with flying lead base
- G Selected for gating.
- K Photomultiplier supplied capped.
- KFL As FL but with a temporary base for subsequent removal or positioning on installation.
- M Supplied with spectral response printout.
- Q Variant with quartz (fused silica) window.
- S Electrostatic and magnetic shielding protected by a black plastic insulating sleeve.
- X Low background glass.

	Characteristics						Features																				Applications								
Type	Spectral response	Diameter mm	CsSb	BeCu	Stages	Multiplier	Low background window	Quartz window for UV (option)	MgF$_2$ window for VUV	High gain	Extended linearity	Single electron resolution	NaI (Tl) resolution	Low rate effect	High speed, large bandwidth	High temperature	Rugged	Compact	Low dark current/count	Gateable	Housing available	Low cost voltage divider	Magnetically screened option	Gamma spectroscopy/counting	Photon counting	Emission spectroscopy	Absorption spectroscopy	Pollution monitoring	Fluorescence spectrophotometry	Colour scanner	Bio/Chemiluminescence	Radio immuno assay	Severe environment	Liquid scintillation counting	High light level	High energy physics, Astrophysics
9423	CsI	52		•	14	LF		•	•	•	•								•	•	•	•	•			•								•	•
9425	RbTe	52		•	14	LF		•	•	•	•								•	•	•	•	•			•								•	•
9426	Bialk	52		•	14	LF		•	•	•	•	•							•	•	•	•	•			•								•	•
9427	S20	52		•	14	LF		•	•	•	•									•	•	•	•			•								•	•
9524	S11	30	•		11	BG	•	•		•				•							•	•	•					•							
9558	S20	52	•		11	VB	•	•		•				•							•		•				•			•					
9659	S20	52	•		11	VB	•			•				•							•		•				•	•		•					
9727	H Bialk	52		•	13	VB	•			•			•			•	•		•		•			•								•			
9782	Bialk	90	•		11	VB		•		•				•				•					•	•											
9780	Bialk	SW	•		9	CF		•						•	•			•	•		•					•	•							•	
9781	Bialk	SW	•		9	CF								•	•			•	•		•					•	•		•	•				•	
9783	Bialk	SW	•		9	CF		•						•	•			•	•		•					•	•		•					•	
9785	Trialk	SW	•		9	CF		•						•	•			•			•					•	•			•				•	
9792	Bialk	130	•		9	VB	•						•	•					•					•											
9794	Bialk	SW	•		8	CF		•						•	•			•	•		•					•	•							•	
9798	S20	30	•		11	BG	•	•		•		•		•							•	•	•				•								
9807	Bialk	52		•	12	LF	•	•		•	•	•			•					•	•	•	•	•	•										•
9813	Bialk	52		•	14	LF	•	•		•	•	•	•		•					•	•	•	•	•	•										•
9814	Bialk	52		•	12	LF	•	•		•	•	•	•		•					•	•	•	•	•	•										•
9816	S20	52		•	14	LF	•	•		•	•	•			•					•	•	•	•	•	•										•
9817	S20	52		•	12	LF	•	•		•	•	•			•					•	•	•	•	•											•
9821	Bialk	78		•	12	LF	•	•		•	•	•	•		•					•	•	•	•	•	•										•
9822	Bialk	78		•	10	LF	•	•			•	•	•		•					•	•		•	•	•										•
9823	Bialk	130		•	14	LF	•	•		•	•	•	•		•					•	•		•	•	•										•
9826	Bialk	19	•		12	LF		•		•	•		•	•	•			•	•		•		•	•	•		•								•
9828	S20	30	•		11	BG				•				•							•	•	•				•	•	•						
9829	Bialk	52		•	12	LF	•	•		•	•	•			•				•	•		•	•		•									•	
9850	S20	52		•	8	LF		•			•				•						•		•							•				•	
9883	S20	52		•	14	LF	•	•		•	•				•				•		•	•	•		•	•									
9889	Bialk	52	•		8	LF	•	•			•	•		•	•			•	•				•											•	
9878	H Bialk	30		•	11	BG	•						•			•	•		•		•		•		•							•			
9879	S20	52		•	12	LF	•	•		•	•	•			•					•		•	•		•	•			•						
9882	S20	19		•	10	LF					•				•			•			•		•		•	•			•						
9888	H Bialk	30		•	11	BG	•						•			•	•		•		•	•	•		•							•			
9893	Bialk	52		•	14	LF	•	•		•	•				•				•		•		•		•	•									
9899	Bialk	52	•		12	LF	•	•		•	•	•		•	•				•				•		•									•	
9900	RbCs	30	•		11	BG	•			•		•	•	•					•			•			•	•									
9902	RbCs	38	•		10	LF	•	•			•	•	•	•	•				•		•		•		•						•				
9903	RbCs	38		•	10	LF	•	•			•	•	•		•				•		•		•		•						•				•
9908	H Bialk	30		•	11	BG	•						•			•	•		•		•		•		•							•			
9921	Bialk	78	•		12	LF	•	•		•	•	•	•	•	•				•				•		•										•
9924	RbCs	30	•		11	BG	•	•		•			•	•					•		•		•		•	•	•		•		•	•			
9954	RbCs	52		•	12	LF	•	•		•	•	•			•					•	•		•		•										•
9956	RbCs	52	•		10	VB	•	•					•	•					•				•		•										
9957	RbCs	52	•		11	VB	•	•		•			•	•									•		•										
9972	S20	38	•		10	LF	•	•			•	•		•	•								•			•	•								
9974	Bialk	HEX		•	10	LF	•				•	•			•				•																•

NUMBER SUFFIX – Customer specific selection

In addition to a letter suffix, a numeric suffix in the range 01 to 99 is used to identify a more stringent specification, which is within the standard published limits and which is customer specific.

EXAMPLES

9102B	standard published specification
9102KB	capped
9102KBE	capped including electrostatic shield
9102QB	variant with quartz window
9102B03	selected to customer specification 03
9102KBFL	temporary cap on flying leads

52 MM (2") DIAMETER 10 STAGE

Electrical Characteristics and Ratings

	PHYSICAL CHARACTERISTICS			CATHODE SENSITIVITY								ANODE SENSITIVITY					DARK EMISSION AT NOMINAL A/lm			
Type	Spectral response	Dynodes	Effective cathode size mm	µA/lm		Corning blue		Corning red		Infra red		QE% peak	A/lm	V_{k-a}	V_{k-a}	Gain x10^6	I_a(dark) nA		Count s^{-1}
			nom	min	typ	min	typ	min	typ	min	typ	typ	nom	typ	max	nom	typ	max	typ
9266B	Bialk	10LF CsSb	45		80	9	12		1.5			28	50	900	1100	0.6	0.2	1.5	300
9250B	Bialk	10LF CsSb	45		80	7	12		1.7			28	50	820	1150	0.6	0.1	1	300
9205B	Bialk	10LF CsSb	45		80	7	12		1.5			28	200	1000	1350	2.5	0.5	20	300
→ 9256B	RbCs	10LF CsSb	45		110	7	12		10			27	50	850	1000	0.5	0.2	1.5	500
9257B	RbCs	10LF BeCu	45		110	7	12		10			27	50	1020	1500	0.5	0.2	1.5	500
9956B	RbCs	10VB CsSb	45		90	7	11		4			26	50	900	1150	0.6	0.2	1.5	400

Series characteristics

Most of the photomultipliers in this series have linear focused dynodes, which provide high speed, wide dynamic range and good linearity. They have a first dynode which is designed to ensure good photoelectron collection and hence excellent pulse height resolution.

These photomultipliers have low background windows. Quartz (fused silica) windows for extended UV response are also available as an option. Most are available in hard pin, flying lead with temporary B14 cap or permanent B14 cap options; with suffix B, KBFL and KB respectively. 9205, 9250 and 9956 are available in B and KB versions only. They can be supplied with a conductive coating and insulating, black plastic sleeve (add 0.8 mm to published diameter). An integral mu-metal shield is also available.

- **9266 (parent type)**
  This is a high gain photomultiplier for scintillation spectroscopy. Typical pulse height resolution figures obtained with a NaI(Tl) test crystal are: ^{137}Cs=7.3%; ^{57}Co=10.5%. This tube has excellent stability versus changing temperature, count rate and time. A detailed technical data sheet is available.
- **9250**
  This type supersedes the earlier 9750 for use in thermo-luminescent dosimetry, liquid scintillation counting and other low light level applications.
- **9205**
  This is an alternative to the 6097 and 9957 venetian blind photomultipliers and can replace them in existing equipment.
- **9256**
  The 9256 is a version of the 9266 with a rubidium bialkali photocathode for increased green response. Typical pulse height resolution obtained with a NaI(Tl) test crystal and a ^{137}Cs source is 7.4%.
- **9257**
  This photomultiplier is a lower gain version of the 9256 with BeCu dynodes. The consequent higher operating voltage improves linearity and timing.
- **9956**
  This photomultiplier is an earlier type for scintillation counting. It has a rubidium bialkali photocathode with good green response and high gain venetian blind dynodes.

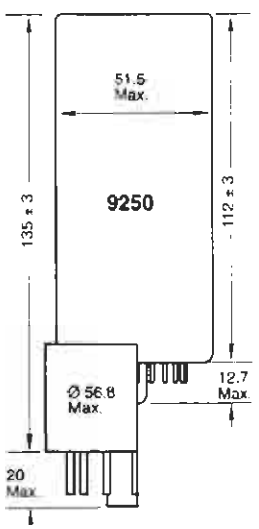

Type	SER	TIME RESPONSE ns				RATINGS - subject to not exceeding maximum rated A/lm						VOLTAGE DIVIDER
	p/v	Rise time	Pulse width (fwhm)	Transit time	Jitter (fwhm)	A/lm	V_{k-d1}	V_{d-d}	V_{k-a}	I_k nA	I_a µA	Distribution used
	typ	typ	typ	typ	typ	max	max	max	max	max	max	See Page 62 #
9266B	2.0	4	5.5	37	5.9	500	300	300	2000	50	100	B
9250B	2.0	4	6.5	42	5.9	500	300	300	1800	100	200	B
9205B	2.0	4	6.6	39	5.9	2000	300	300	1800	100	200	B
9256B	2.0	4	6.6	39	5.9	500	300	300	1800	100	200	B
9257B	2.0	3.5	5	35	5	500	300	300	1800	100	200	B
9956B		12	25	65		500	300	300	2000	50	200	E

Spectral Response

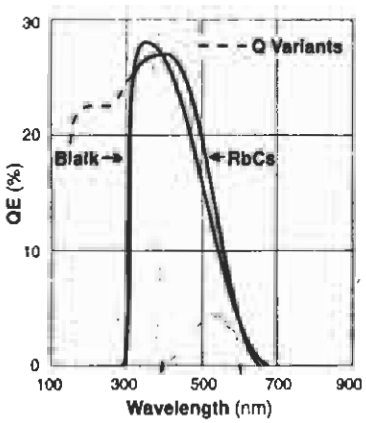

Gain Curves

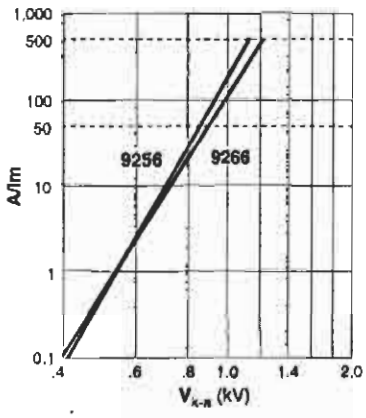

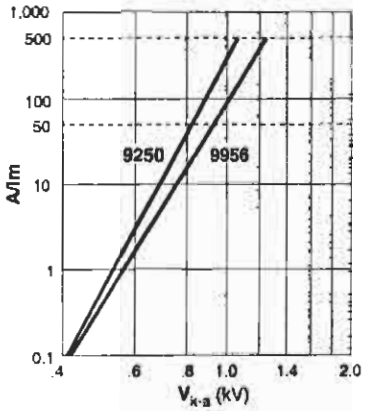

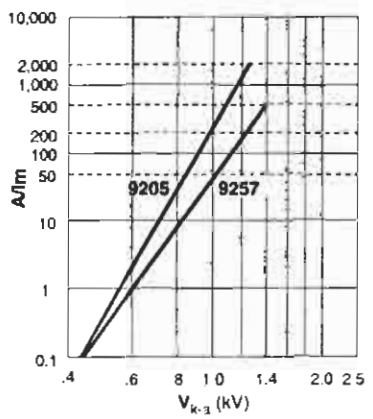

Pin connections

(Viewed from below. V indicates position of short pin or key; ic = internal connection).
The corresponding socket type number is shown below each diagram.

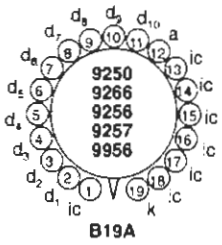

B19A

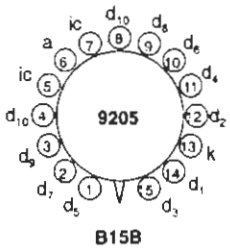

B15B

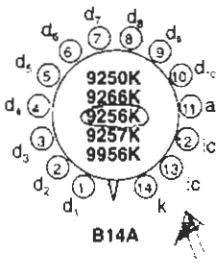

B14A

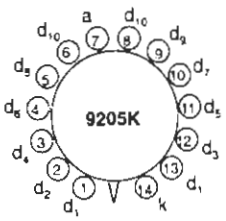

B14A

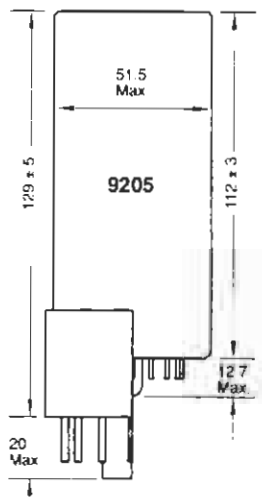

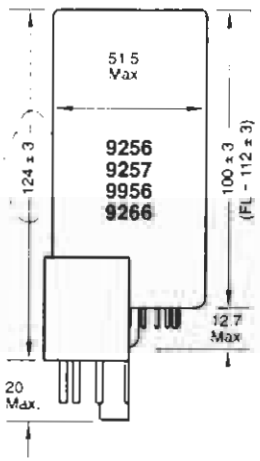

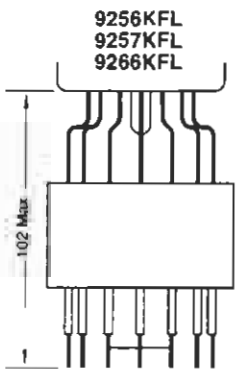

THORN EMI Standard Voltage Dividers for Performance Specification

Test ticket data and electrical specifications contained in the tables of pages 26 to 56 refer to measurements made with the voltage dividers listed on this page. Where a photomultiplier has a focus electrode, f, this is connected to d_1 except for type 9823, where f-d_1 is maintained at 30% of k -d_1 voltage. For 9353K connect focus to d_3.

The standard voltage dividers are not necessarily optimum and advice should be sought from THORN EMI for new applications. The use of non-standard voltage dividers will affect performance. In particular:

- anode sensitivity
- dark emission
- time response

may be different from that stated on the rest ticket or given in the electrical characteristics of rhis catalogue. With non-standard dividers particular care must be exercised to ensure that photomultiplier ratings are never exceeded.

Decoupling capacitors are used on the last three dynodes, as appropriate.

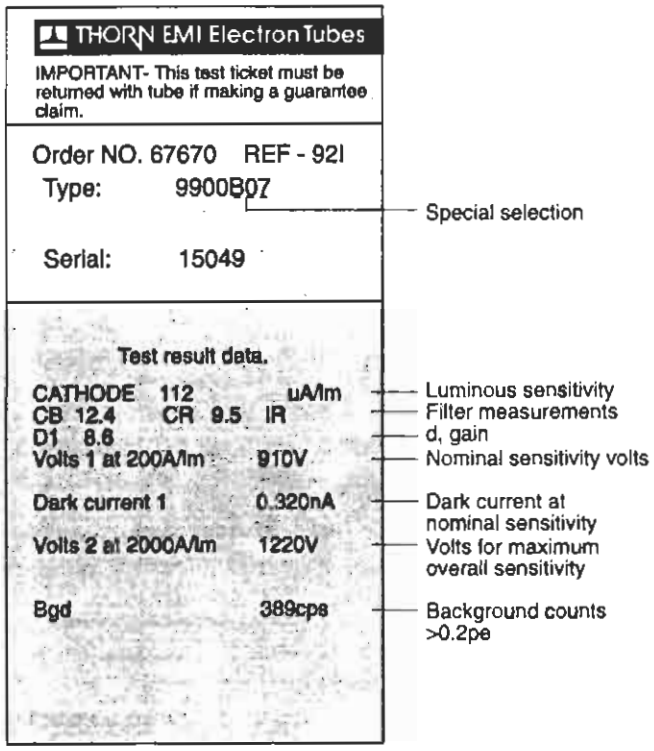

Ref	k	d_1	d_2	d_3	d_4	d_5	.....	d_{n-5}	d_{n-4}	d_{n-3}	d_{n-2}	d_{n-1}	d_n	a	Ref
A	1.5R	R	R	R	R	R	.....	R	R	R	R	R	R		A
B	2R	R	R	R	R	R	.....	R	R	R	R	R	R		B
C	2R	1.5R	1.5R	R	R		.....	R	R	R	R	R	R		C
D	3R	R	R	R	R	R	.....	R	R	R	R	R	R		D
E	150V	R	R	R	R		.....	R	R	R	R	2R	R		E
F	150V	R	R	R	R		.....	R	R	R	R	R	R		F
G	300V	R	R	R	R		.....	R	R	1.25R	1.5R	2R	3R		G
H	300V	R	R	R	R		.....	R	R	R	R	R	R		H
I	600V	R	R	R	R		.....	R	R	R	R	R	R		I
J	300V	R	R	R	R		.....	R	R	R	R	2R	R		J
K	450V	R	R	R	R		.....	R	R	1.25R	1.5R	2R	3R		K
L	450V	R	R	R	R		.....	R	R	R	R	R	R		L
M	450V	R	R	R	R		.....	R	R	R	R	2R	R		M
N	4R	R	2R	R	R		.....	R	R	1.25R	1.5R	2R	3R		N
O	8R	2R	1.5R	R	R		.....	R	1.5R	2R	3R	4R	3R		O
P	450V	1.5R	1.5R	R	R		.....	R	R	R	R	R	R		P
R	2R	1.5R	R	R	R		.....	R	R	R	R	R	R		R
S	R	R	R	R	R		.....	R	R	R	R	R	R		S

The THORN EMI Approach

THORN EMI offers technical assistance based on many years of experience in the design and use of photomultipliers. Customers are invited to contact us at the design stage of their project and we will maintain close co-operation through to product release. Our range of accessory items allows the scientist and engineer to achieve objectives reliably, at reasonable cost and, most importantly, quickly. THORN EMI is always ready to discuss adaptation of standard products, used in the prototype stage, for production volume requirements.

A photomultiplier is an extremely sensitive light detector which demands particular care and skill in its installation and use. To perform the primary function of converting a light signal into an electrical analogue needs application of high voltage within an electrically screened environment and a housing, such as that of Figure 39, to exclude extraneous light while providing tube support and location in a safe manner. In addition, optimum handling of photomultiplier signals needs attention to electrical insulation, impedance matching and adoption of good high frequency techniques. Recognition of these requirements is part of THORN EMI's design policy of continually improving the product range.

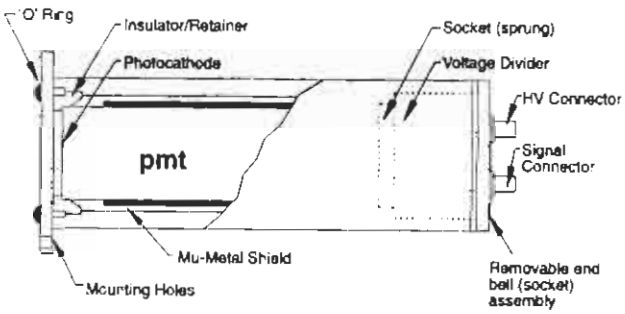

Figure 39

Illustrating the construction details and critical points in the design of a photomultiplier housing.

Photomultiplier Configurations

In its most basic form, shown in Figure 40(a), electrical contact to the photomultiplier is through a series of metal pins arranged in a circle on the base of the envelope. A capped tube has a more substantial pin-out culminating in a light-tight, plastic cap. The cap may be loosely fitted, as in Figure 40(b) to allow the user to position the cap into a tubular housing or, as shown in 40(c), with the cap firmly attached to the photomultiplier envelope.

Photomultipliers are available with screened envelopes. Figure 40(d) shows electrostatic and 40(e) combined electrostatic and magnetic screening. In both cases the screening material is enveloped in a light tight, insulating sleeve. Note also that the base of the photomultiplier can be supplied painted or covered with an elastomer to exclude light. A complete package

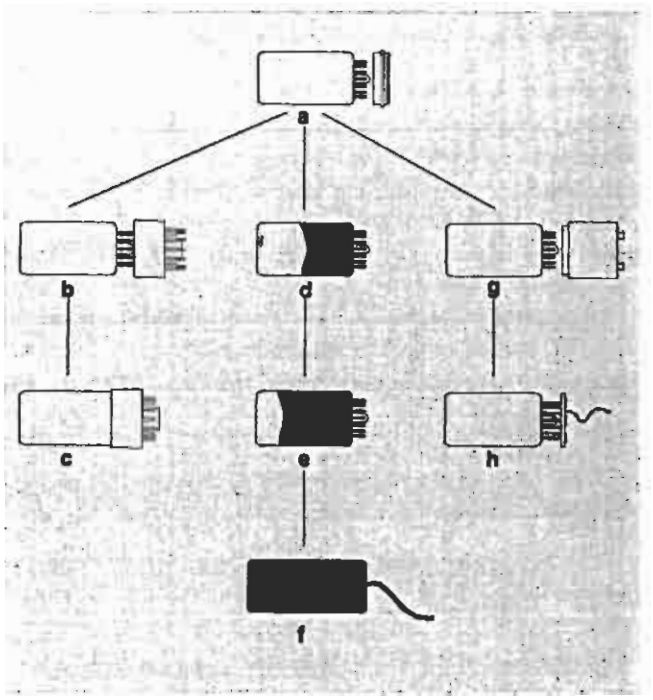

Figure 40

Pin-out and voltage divider options.

consisting of a magnetically screened, light-tight enclosure with integral divider, is illustrated in 40(f). Please discuss your particular requirements with THORN EMI.

THORN EMI provides sockets wired with discrete components 40(g) or thick film networks for direct fitting to tubes with flying leads, 40(h).

Photomultiplier Housings

THORN EMI has a comprehensive range of ambient and cooled housings suitable for the entire range of side window and 19 mm, 38 mm and 52 mm end window photomultipliers. Amplifiers, gating circuits and amplifier-discriminators can be incorporated within a housing, providing ideal matching and a minimum of electrical pick-up.

The question of whether to cool and stabilise the temperature of a photomultiplier is based on two considerations. The application is background limited or the photomultiplier sensitivity variation, because of temperature change, is critical. The curves of Figure 23 (page 15) illustrate the reduction in background attainable by cooling. However, the results of Figure 29 (page 18), representing the change in cathode sensitivity, point to a compromise between the benefits of reduced background and the loss of red sensitivity with increased cooling.

Electrostatic and Magnetic Screening

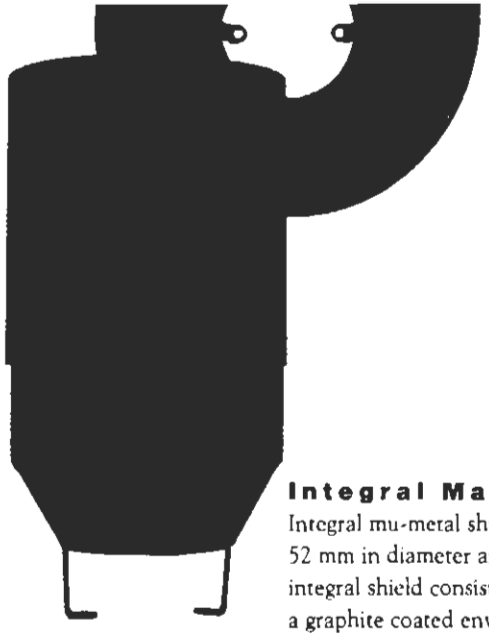

Electrostatic Shielding

All photomultipliers of diameter 52 mm or less can be supplied with a conductive coating on the envelope, connected to the cathode pin. An insulating sleeve covers this coating, for safety reasons, adding 0.8 mm to the published photomultiplier diameter. Refer to Section 6.3 in rhis catalogue for a full account of the effect of exrernal electric fields on tube performance.

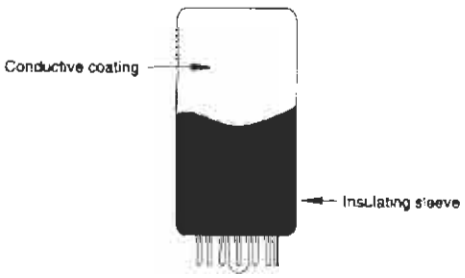

Magnetic Shielding

Section 6.2 of the catalogue discusses the effects of stray magnetic fields on photomultiplier performance. Where modest fields are concerned, the 'Integral', low cost, thin shields are usually sufficient. For harsher electro-magneric environments, separate shields of 0.5 mm thickness — the MS Series, are recommended.

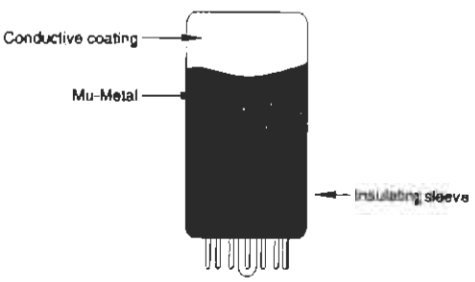

Integral Magnetic Shields

Integral mu-metal shields for end window photomultipliers up to 52 mm in diameter are available. A photomultiplier with an integral shield consists of 0.05 mm of mu-metal wrapped around a graphite coated envelope and electrically protected by an insulating sleeve. The graphite and mu-meral are connected to the cathode pin. Photomulripliers which incorporate a wrapped shield are designated by the suffix S, for example 9125S.

Separate Magnetic Shields

The MS series of discrete mu-metal shields are profiled to the outline of the photomultiplier. They are available for photomultipliers ranging from 19 to 190 mm in diameter.

Table 1 Split cylinder shields with internal grip pad. Shields are 0.5 mm rhick wirh the ourline shown below.

Type	Length A (nom)	Diameter B (nom)	Photomultiplier Diameter (mm)
MS19A	75	22	19
MS30A	76	33	30
MS30B	102	33	30
MS38A	83	41	38
MS52A	76	56	52
MS52B	102	56	52
MS52C	133	56	52
MS52D	152	56	52

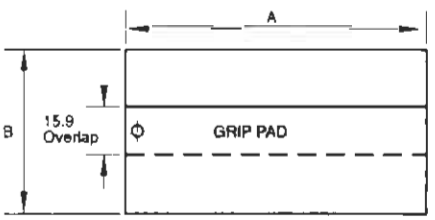

Table 2 Solid cylindrical shields.

Type	Length (mm)	Diameter (mm)	Wall (mm)	Photomultiplier Diameter (mm)
MS30C	120	34	1	30
MS52G	208	60	2	52

Table 3 Contoured shields. Mounting lugs to fit the flanges of the sockets indicated.

Type	Photomultiplier Diameter (mm)	Socket
MS SW	30(SW)	No Lugs
MS52E	52	B14A, B21
MS52F	52	B15B, B19A
MS75/90	75	B15B, B19A
MS75/90	90	B15B, B19A
MS130A	130	B15B
MS190A	190	B15B

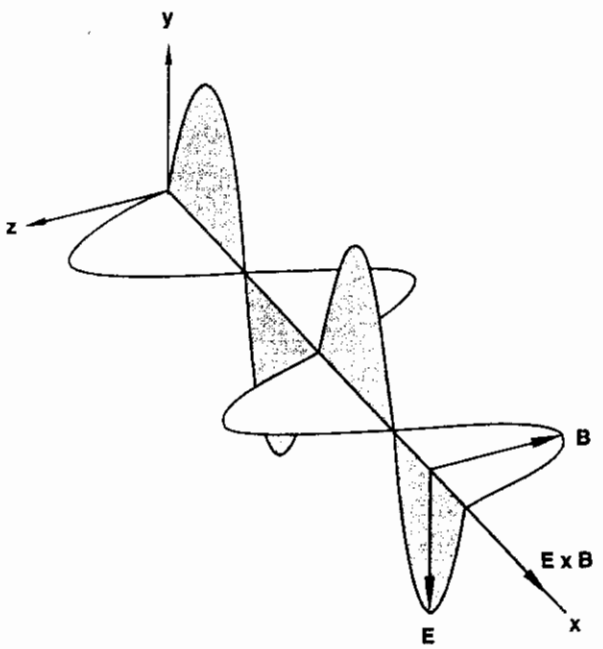

Dimensions mm

MSSW

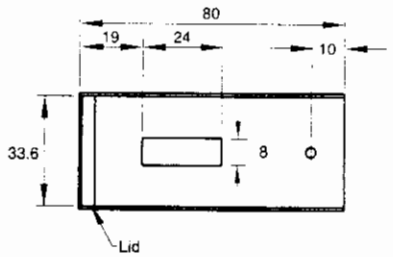

MS52E

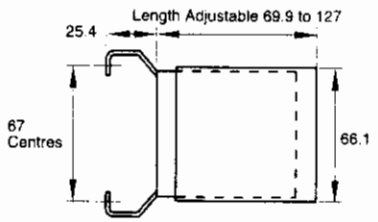

MS52F

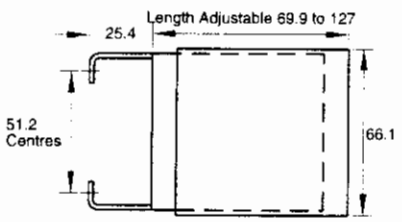

MS75/90

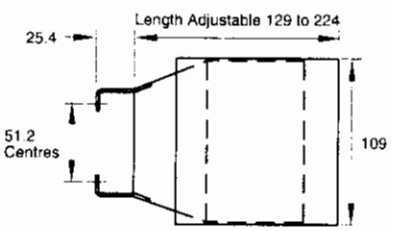

MS130A

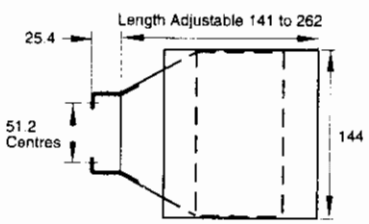

MS190A

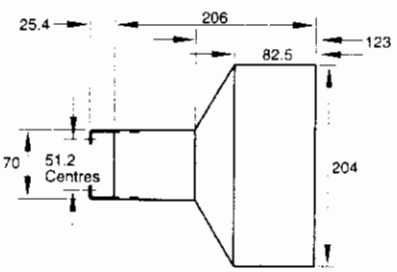

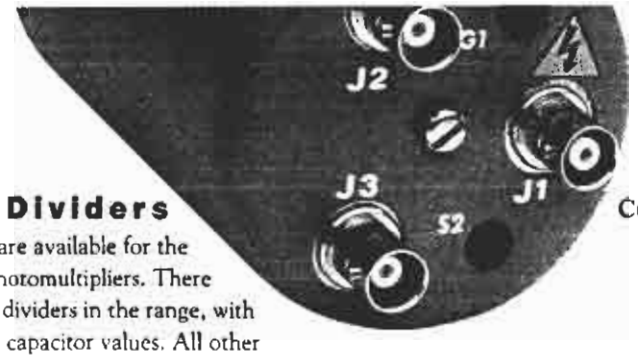

Voltage Dividers

Voltage dividers are available for the entire range of photomultipliers. There are two standard dividers in the range, with fixed resistor and capacitor values. All other dividers are manufacrured ro customer specification.

The C637 and C638 are the first in a new series of thick film dividers aimed parricularly at large volume users. The TB series are active dividers which use transistors to provide performance free from rate effect (See Section 8.2). Unenclosed, wired sockets to customer specification are offered over the entire range — these are designated C610. Wired sockets in a range of metal and plastic enclosures are available in the RB and TB series or as C611, C613 and C623.

C610 Available for any flanged socket type with user specified resistor and capacitor network. Skeleton construction with flying leads.

C637 For all 11 stage, 1⅛" photomultipliers. Available as: i) free board, C637; ii) B14B socket mounted, C637/14; iii) flanged B14B socket mounted, C637/14F. As supplied links L_1 to L_4 are intact — alternative options may be realised by removal of these links.
— **HV:** ground T_1, remove L_5, apply —HV to pin 13.
+ **HV:** ground pin 13, apply +HV to T_1 and add C_4.

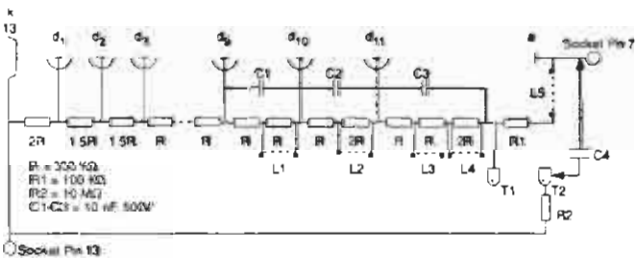

C638 For all 2", 3" and 5" fast tubes. Available as: i) free board, C638; ii) B19A socket mounted, C638/19; iii) flanged B19A socket mounted, C638/19F. The divider is manufactured with links L_1 to L_9 intact — alternative configurations may be realised by removal of these links. The divider interfaces ro a GB1 gating board through use of links L_3 to L_5. Ground plane construction minimises ringing and pulse distortion.
— **HV:** ground T_4, remove L_{10}, apply —HV to T_1.
+ **HV:** ground T_1, apply +HV to T_4 and add C_3.

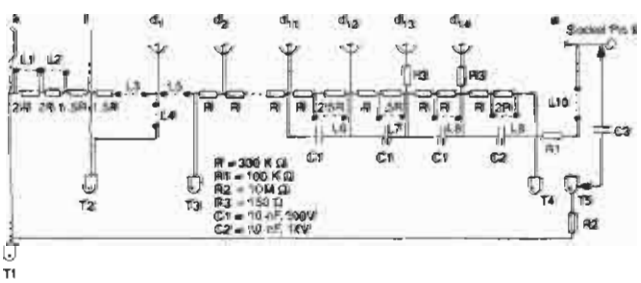

C611 B14B socket in tubular plastic case with flying leads for high voltage and signal outputs.

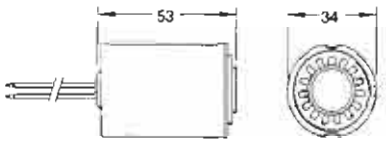

C613 Available with B11A, B12A, B14B, B15B or B19A socket encapsulated in rectangular plastic box. MHV connector for high voltage and BNC for signal ourput.

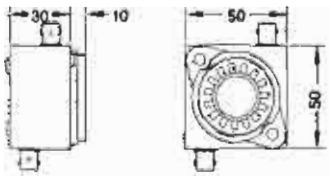

C623 B11A socket encapsulated in tubular metal case with flying leads for high voltage and signal outputs.

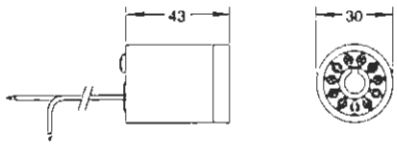

RB/TB This series has a divider within a metal enclosure. RB refers to resistive dividers. The TB range uses transistors for high transient anode currents. BNC outputs from the anode and the last dynode are provided.

Base Type	TB Series	RB Series
B19	TB1102	RB1102
B12	TB1103	RB1103
B21	TB1104	RB1104
B15	TB1105	RB1105
B20	TB1106	RB1106
B14B	TB1107	RB1107
B14A	TB1108	RB1108

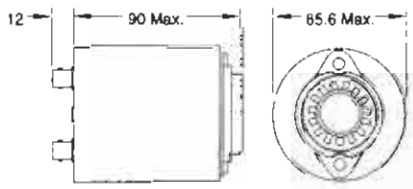

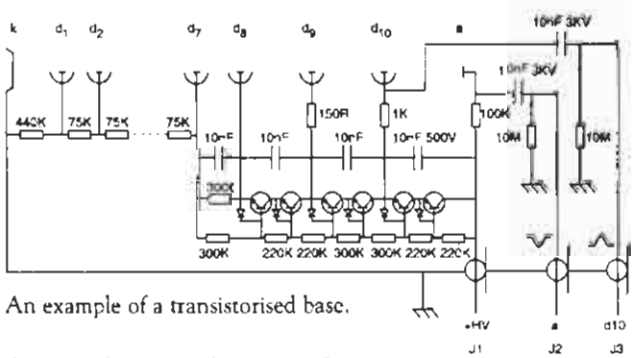

An example of a transistorised base.

Ordering Information

When ordering a wired socket please state voltage divider type number, tube type, HV polarity and application.

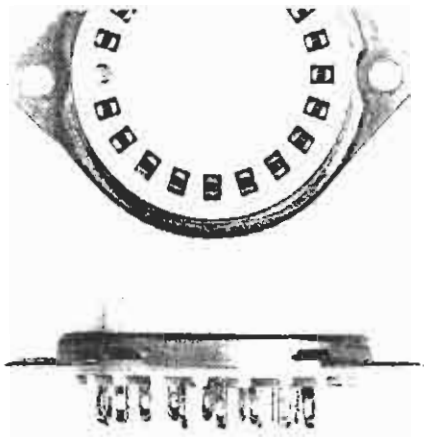

Photomultiplier Sockets

Precautions for optimum performance

All photomultipliers with hard-pin or overcapped bases require a matching socket to enable external connections to be made. Components fixed to the socket must not interfere with or distort the natural pitch circle diameter of the contacts. The tube pins must not be modified. In particular, soldering directly to the pins will invalidate the guarantee. Socket pins corresponding to ic connections, shown in the photomultiplier pin connection diagrams, must not be used. When inserting or removing a photomultiplier from the socket, maintain the tube perpendicular to the plane of the socket and avoid undue force.

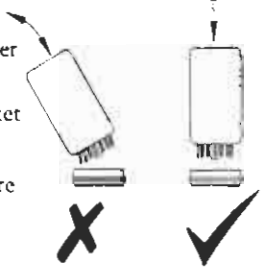

THORN EMI sockets and overcaps are made from highly insulating, thermoplastic materials.

- soldering temperatures must not exceed 220 °C
- sockets or over-caps must not be allowed to come into contact with the following: acetone, cyanoacrylate adhesives ('Super glue'), chloroform, dichloromethane (paint stripper)
- suitable adhesives for this material are: epoxy resins ('Araldite'), polyurethane glue and silicones
- the surface must be cleaned prior to bonding — alcohol is recommended

Ordering Information

Standard sockets are fitted with mounting flanges. Unflanged versions with standard or pcb contacts are also available (except for B14A and B20).

Order Code	Description
B11A	11 contacts on 19.05 mm pcd
B12A	12 contacts on 27.0 mm pcd
B12D	12 contacts on 12.7 mm pcd
B14A	14 contacts on 44.45 mm pcd, includes cover
B14B	14 contacts on 19.05 mm pcd
B15B	15 contacts on 31.75 mm pcd
B19A	19 contacts on 31.75 mm pcd
B20	with separate 90 mm flange with three 4 mm mounting holes symmetrically spaced on 82 mm pcd. 20 contacts on 44.45 mm pcd.
B21	21 contacts on 34.90 mm pcd

Add suffix LF to order a socket without mounting flange.
Add suffix PC to order a pcb version of a socket.

Dimensions mm

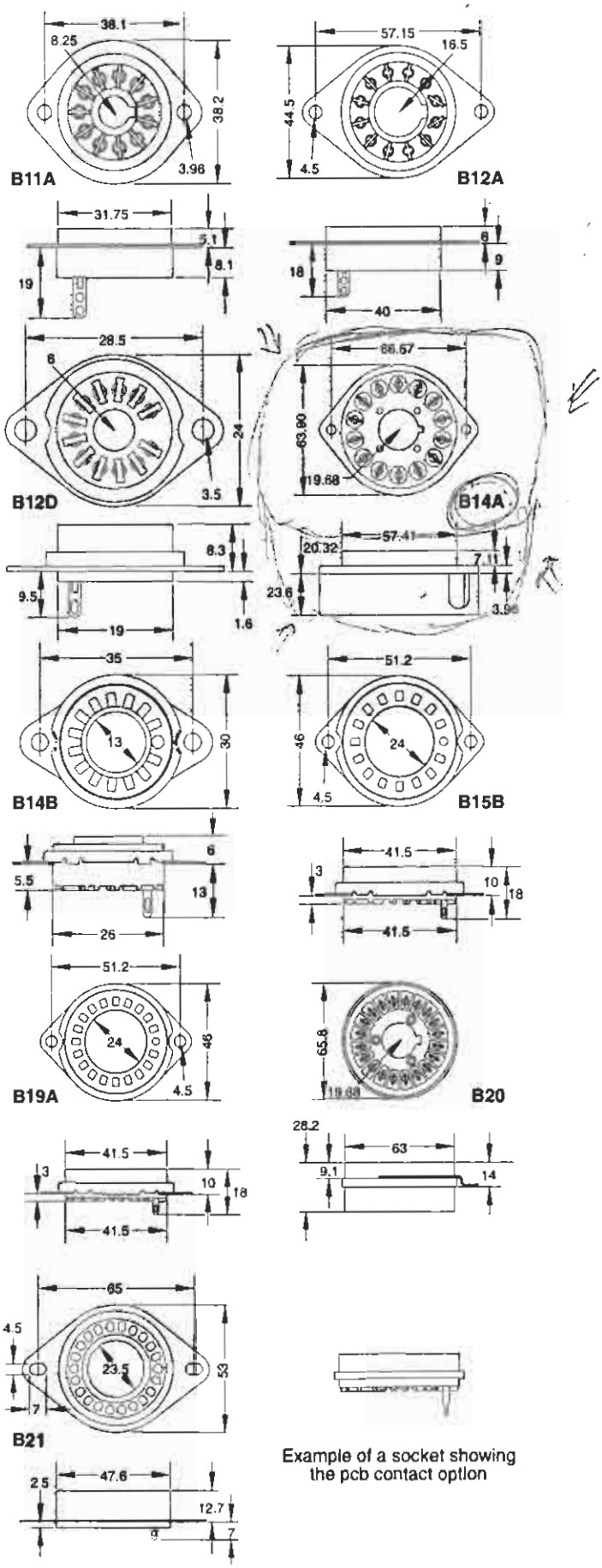

Example of a socket showing the pcb contact option